上海交通大学
SHANGHAI JIAO TONG UNIVERSITY

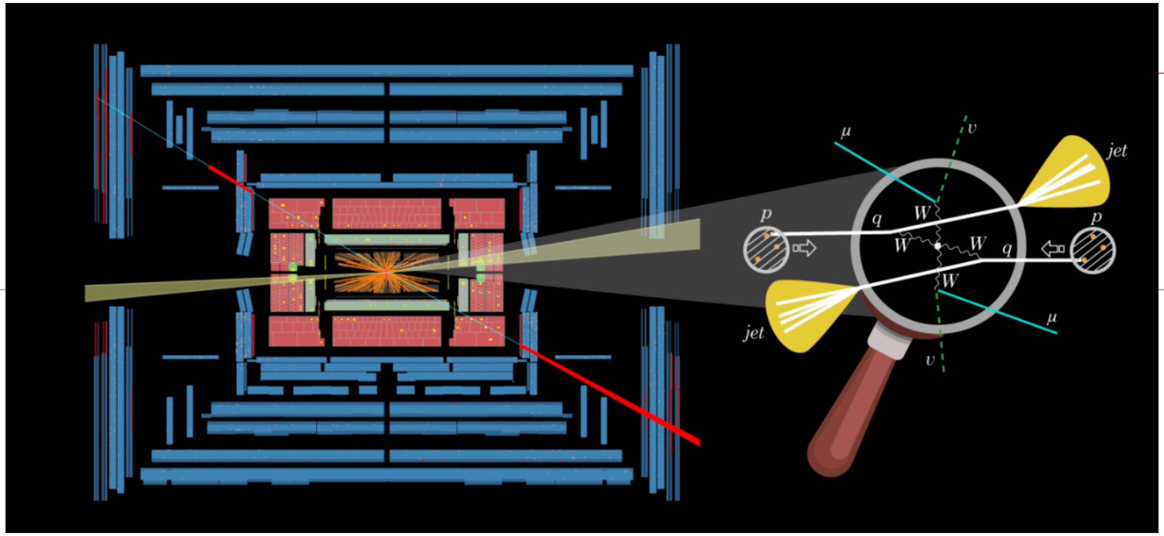

Measurements of vector-boson scattering with the ATLAS experiment

Xi Wang
On behalf of ATLAS

ICHEP, 20 Jul 2024, Prague

饮 水 思 源 • 爱 国 荣 校

ATLAS EXPERIMENT

Contents

- Vector boson scattering physics at ATLAS in a nutshell
- Recent VBS measurement progresses at ATLAS
  - $ZZ \rightarrow$ four charged leptons
  - *WZ pair production*
  - *VBS same – sign WW*
  - *VBS opposite – sign WW*
  - *VBS Wγ*
- Summary and prospects

Standard Model Summary Plots June 2024

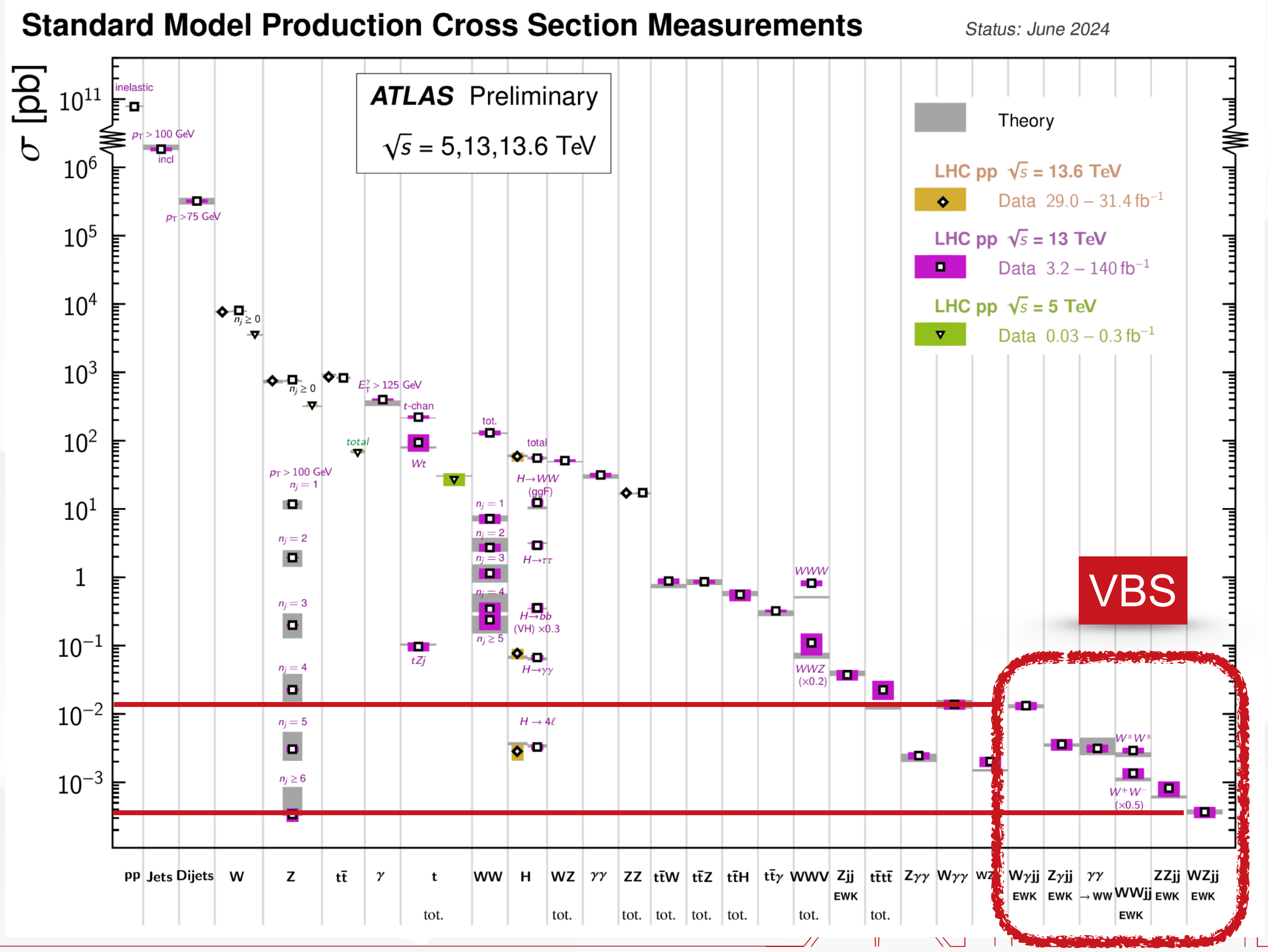

Introduction: Why VBS interesting?

- Test of electroweak sector of the Standard Model (SM) at the TeV scale
- Sensitive to Anomalous Quartic Gauge Couplings(aQGC)
  - Can used to set limits on effective field theory (EFT) operators

$$\mathcal{L}_{SMEFT} = \mathcal{L}_{SM} + \sum_i \frac{c_i}{\Lambda^2} O_i^{(6)} + \frac{c_i}{\Lambda^4} O_i^{(8)} + \ldots$$

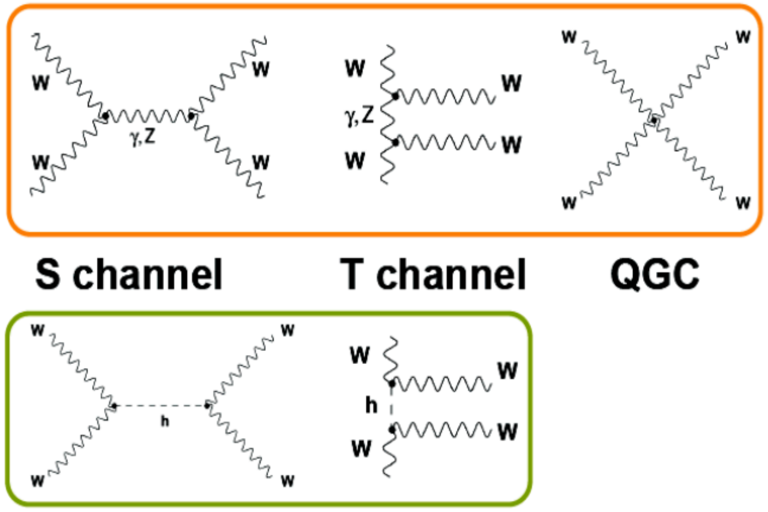

- Measurable key process linked with Electroweak Symmetry Breaking (EWSB)
  - Without a “light” SM Higgs boson ($m_H \leq 1\mathrm{TeV}$) VBS would violate unitarity.

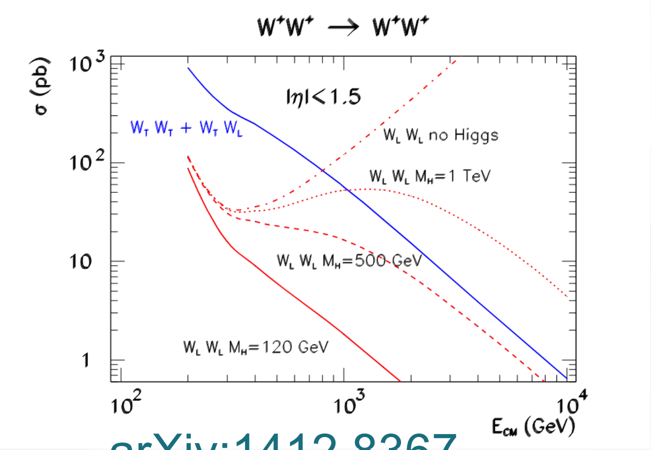

arXiv:1412.8367

$$\mathcal{M}_{\rm SM}(W_L^+W_L^- \to W_L^+W_L^-) \approx \mathcal{M}_{\rm SM}(w^+w^- \to w^+w^-)$$
$$\approx -4\mathrm{i}\lambda - \frac{4\mathrm{i}\lambda^2 v^2}{s - m_H^2} - \frac{4\mathrm{i}\lambda^2 v^2}{t - m_H^2}$$
$$\approx -\mathrm{i}\frac{m_H^2}{v^2}\left[2 + \frac{m_H^2}{s - m_H^2} + \frac{m_H^2}{t - m_H^2}\right]$$

Topology of vector boson scattering

- VBS signature
  - Energetic and forward jets
    - Large **rapidity** separation, $\Delta\eta_{jj}$
    - Large **invariant mass**, M_{jj}
  - Centrality
    - **Low hadronic activity** in the central region(color singlet exchange)
    - Key discrimination for EWK $VV+jj$ and VBS components

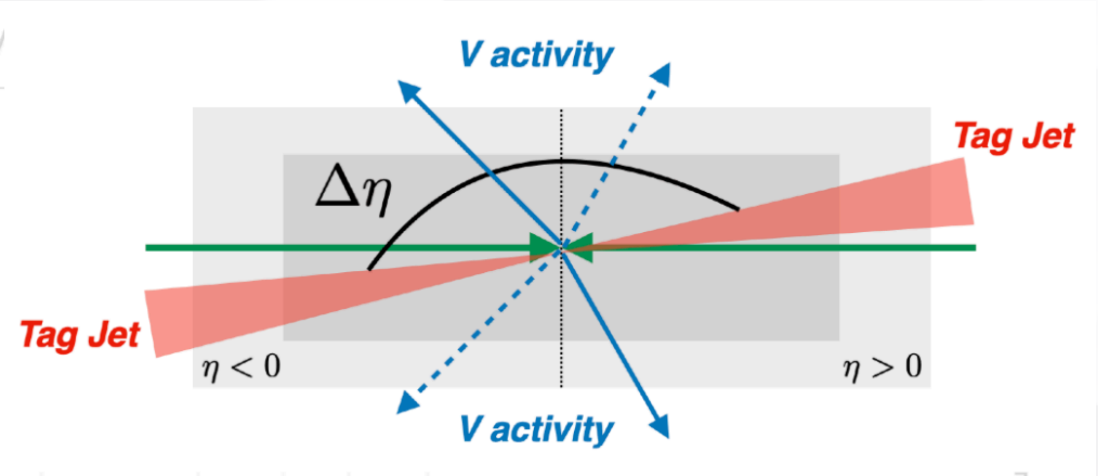

- VBS experimental challenges
  - **Rare process** and large variety of background processes
  - Forward jets identification
  - VBS can not be directly extracted to due gauge invariance
    - → EWK $VV+jj$ in **VBS enhanced phase space**
  - **Interference with QCD** $VV+jj$ production

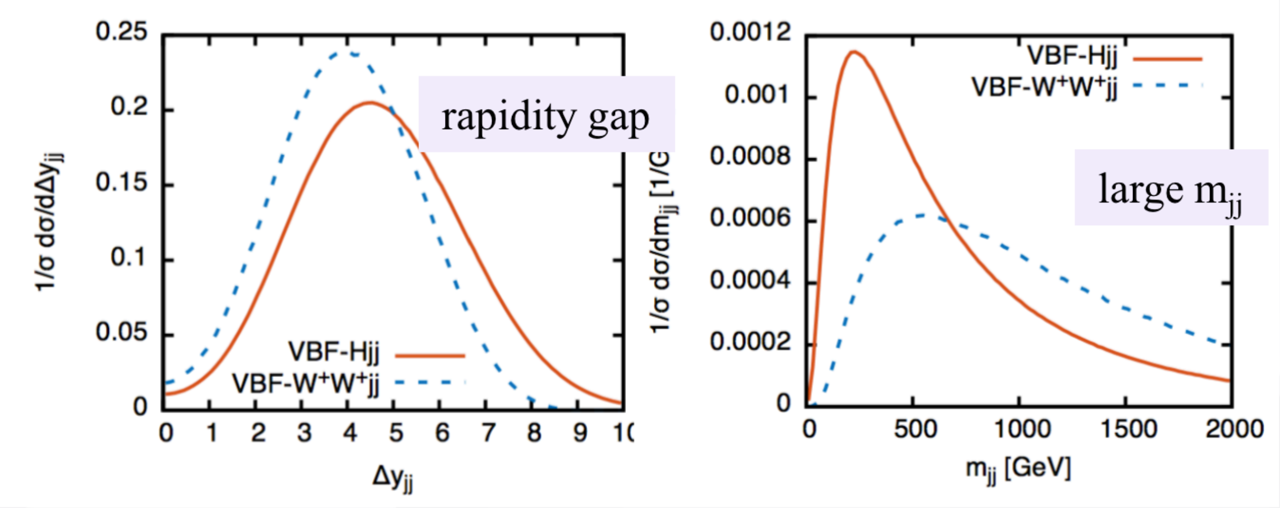

VBS measurement progresses at ATLAS

SM VBS processes in the ATLAS experiment in different channels

Channel	Final state	Luminosity	Date	Journal Reference
$\mathrm{VV+jj}$	$semi-leptonic$	$35\mathrm{fb}^{-1}$	2019-08-22	Phys. Rev. D 100 (2019) 032007
$\gamma\gamma\to\mathrm{WW}(\gamma-\mathrm{induced})$	$e\nu\mu\nu$	$139\mathrm{fb}^{-1}$	2012-05-10	Phys. Lett. B 816 (2021) 136190
$\mathrm{Z}\gamma+\mathrm{jj}$	$\nu\bar{\nu}\gamma+jj$	$140\mathrm{fb}^{-1}$	2022-08-26	JHEP 06 (2023) 082
$\mathrm{Z}\gamma+\mathrm{jj}$	$ll\gamma+jj$	$140\mathrm{fb}^{-1}$	2023-05-30	Phys. Lett. B 846 (2023) 138222
$\mathrm{ZZ+jj}$	$2l2\nu+jj$	$139\mathrm{fb}^{-1}$	2023-02-09	Nature Phys. 19(2023) 237
$\mathrm{ZZ+jj}$	$llll+jj$	$139\mathrm{fb}^{-1}$	2023-11-16	Phys. Lett. B 855 (2024) 138764
$W^{\pm}W^{\pm}+jj$	$l\nu l\nu+jj$	$139\mathrm{fb}^{-1}$	2023-12-01	JHEP 04 (2024) 026
$\mathrm{W^{+}W^{-}+jj}$	$e\nu\mu\nu+jj$	$140\mathrm{fb}^{-1}$	2024-03-07	Submitted to JHEP, arXiv:2403.04869
$\mathrm{W}\gamma+\mathrm{jj}$	$l\nu\gamma+jj$	$140\mathrm{fb}^{-1}$	2024-03-05	Submitted to EPJC, arXiv:2403.02809
$\mathrm{WZ+jj}$	$l\nu ll+jj$	$140\mathrm{fb}^{-1}$	2024-03-22	Accepted by JHEP, arXiv:2403.15296

Today's topics

- Differential cross section for EW $ZZjj$ and strong $ZZjj$ processes are measured to study SM VBS process and access the accuracy of the perturbative QCD calculations.
- Event selection criteria:
  - Two SFOS lepton pairs with smallest $|m_{12} - m_Z| + |m_{34} - m_Z|$
  - Leading pair with highest $|y_{ij}|$, $m_{4l} > 130$ GeV
  - $p_{T,\ j_{1(2)}} > 40(30)$ GeV, $m_{jj} > 300$ GeV, $\Delta Y_{jj} > 2$
  - VBS enhanced region with low centrality ($\xi < 0.4$)
  - VBS suppressed region with high centrality ($\xi > 0.4$)
- Non-prompt background estimated by lepton fake efficiency
  - $Z + jets$(light flavor decays) and $t\bar{t}$(tight flavor decays)
  - $f/(1-f)$ applied to CR with one or more leptons falling to meet the signal lepton definition

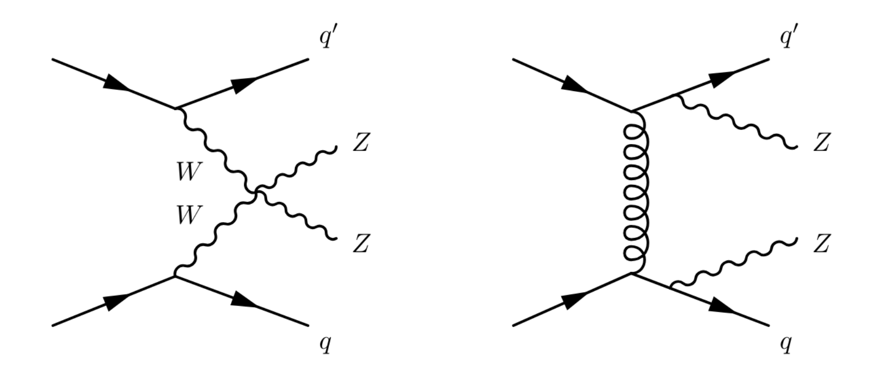

Feynman diagrams for EW $ZZjj$ production (left) and strong $ZZjj$ production (right)

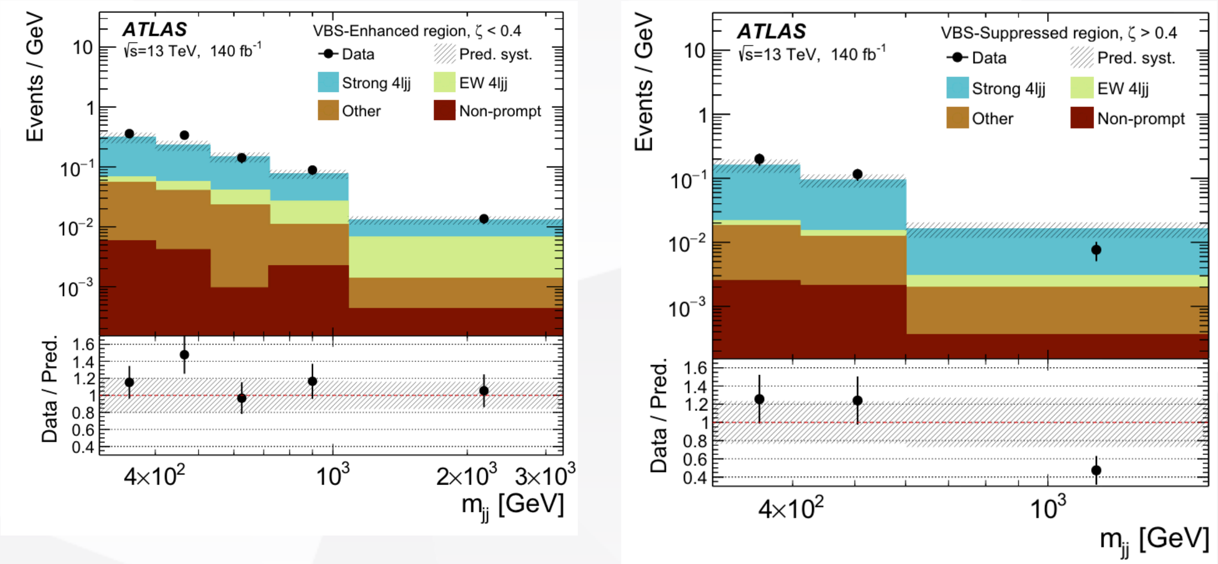

Predicted and observed yields measured in VBS-enhanced region and VBS-suppressed region

ZZ + jj: Differential measurements and EFT

- Differential cross-sections measured in VBS-enhanced and VBS-suppressed regions with various variables
  - VBS observables
  - Polarization, charge conjugation and parity observables
  - QCD-sensitive observables

- Observable m_{4l} and m_{jj} in VBS-enhanced region are used to limit EFT operators

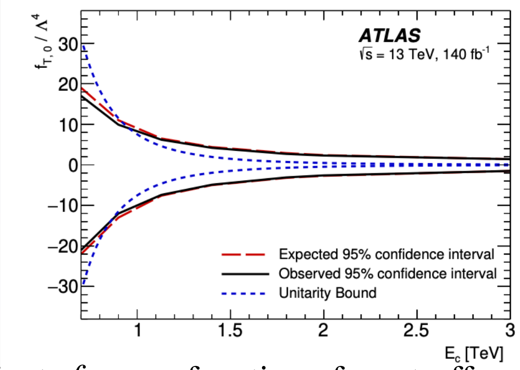

Wilson coefficients $f_{T,0}$ as a function of a cut-off scale, E_c

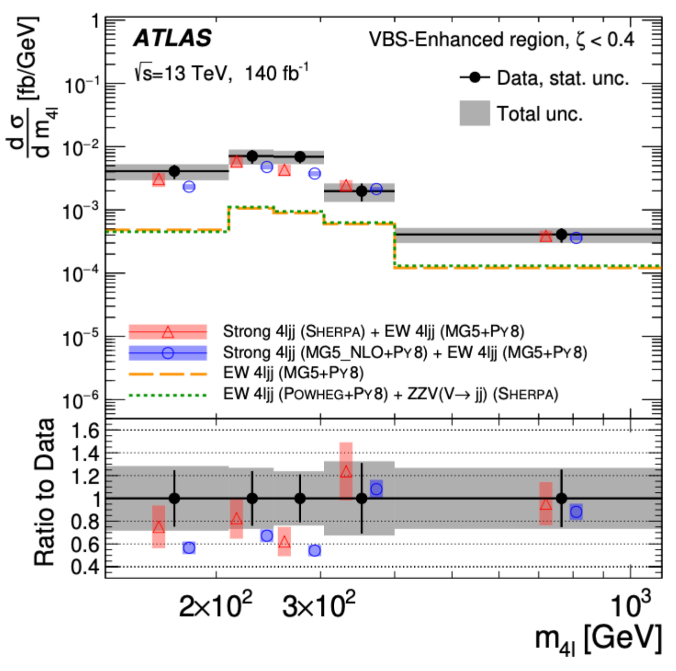

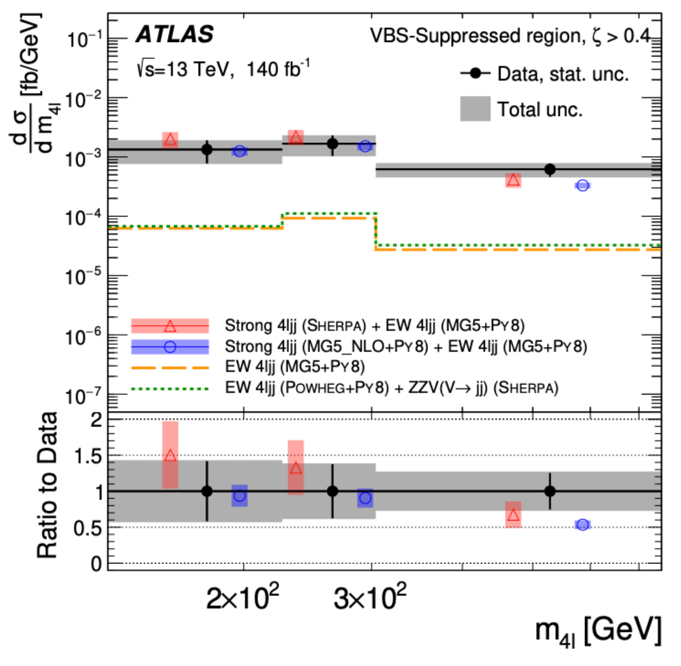

$O_{T,0}$ and $O_{T,1}$ most tightly constrained

Wilson coefficient	$\lvert\mathcal{M}_{d8}\rvert^2$ Included	95% confidence interval [TeV^{-4}] Expected	Observed
$f_{T,0}/\Lambda^4$	yes	[-0.98, 0.93]	[-1.00, 0.97]
	no	[-23, 17]	[-19, 19]
$f_{T,1}/\Lambda^4$	yes	[-1.2, 1.2]	[-1.3, 1.3]
	no	[-160, 120]	[-140, 140]
$f_{T,2}/\Lambda^4$	yes	[-2.5, 2.4]	[-2.6, 2.5]
	no	[-74, 56]	[-63, 62]
$f_{T,5}/\Lambda^4$	yes	[-2.5, 2.4]	[-2.6, 2.5]
	no	[-79, 60]	[-68, 67]
$f_{T,6}/\Lambda^4$	yes	[-3.9, 3.9]	[-4.1, 4.1]
	no	[-64, 48]	[-55, 54]
$f_{T,7}/\Lambda^4$	yes	[-8.5, 8.1]	[-8.8, 8.4]
	no	[-260, 200]	[-220, 220]
$f_{T,8}/\Lambda^4$	yes	[-2.1, 2.1]	[-2.2, 2.2]
	no	[-4.6, 3.1]×10^4	[-3.9, 3.8]×10^4
$f_{T,9}/\Lambda^4$	yes	[-4.5, 4.5]	[-4.7, 4.7]
	no	[-7.5, 5.5]×10^4	[-6.4, 6.3]×10^4

$W^{\pm}W^{\pm}+jj$: Introduction and selections

JHEP04(2024)026

- In the SM, couplings to the Higgs boson prevent the divergence of longitudinally polarised VBS amplitudes at high energies and unitarity violation at the TeV scale
- Background Estimation:

largest ratio of EWK/Strong XS

  - Dominant background comes from $WZ/\gamma^{*}jj$ **(22% SR)**
  - Data-driven method: non-prompt lepton and electron charge misidentification backgrounds
- Event selection criteria:

Reduce Drell – Yan process

Requirement	SR	Low-m_{jj} CR	WZ CR
Leading and subleading lepton p_T		> 27 GeV	
Electron $\|\eta\|$		< 2.47 (1.37 in ee), excluding $1.37 \leq \|\eta\| \leq 1.52$	
Muon $\|\eta\|$		< 2.5	
Leading (subleading) jet p_T		$> 65\,(35)$ GeV	
Additional jet p_T		> 25 GeV	
Jet $\|\eta\|$		< 4.5	
$m_{\ell\ell}$		> 20 GeV	
E_T^{miss}		> 30 GeV	
Charge misid. $Z \to ee$ veto	$\|m_{ee} - m_Z\| > 15$ GeV		–
b-jet veto		$N_{b\text{-jet}} = 0$, $p_T^{b\text{-jet}} > 20$ GeV, $\|\eta^{b\text{-jet}}\| < 2.5$	
$N_{\text{veto leptons}}$	$= 0$	$= 0$	$= 1$, $p_T > 15$ GeV
$m_{\ell\ell\ell}$	–	–	> 106 GeV
m_{jj}	> 500 GeV	$200 < m_{jj} < 500$ GeV	> 200 GeV
$\|\Delta y_{jj}\|$		> 2	

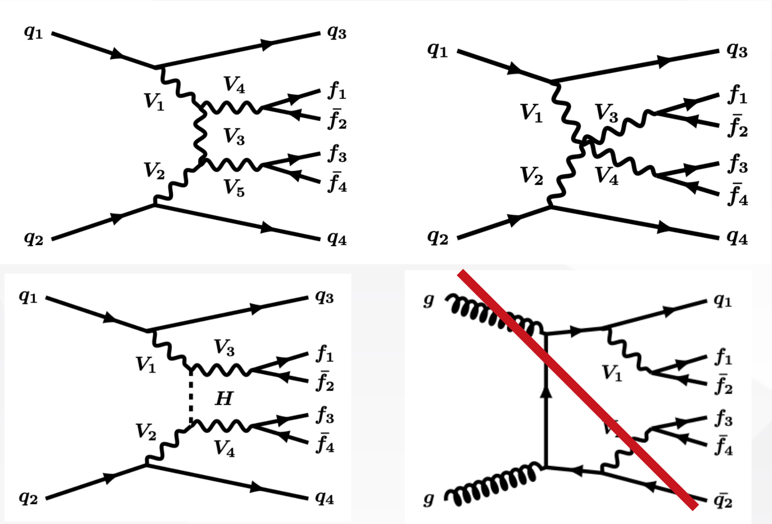

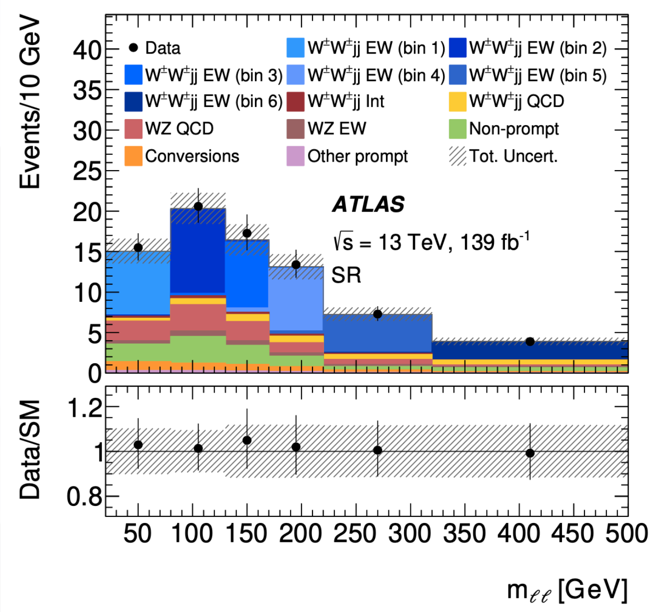

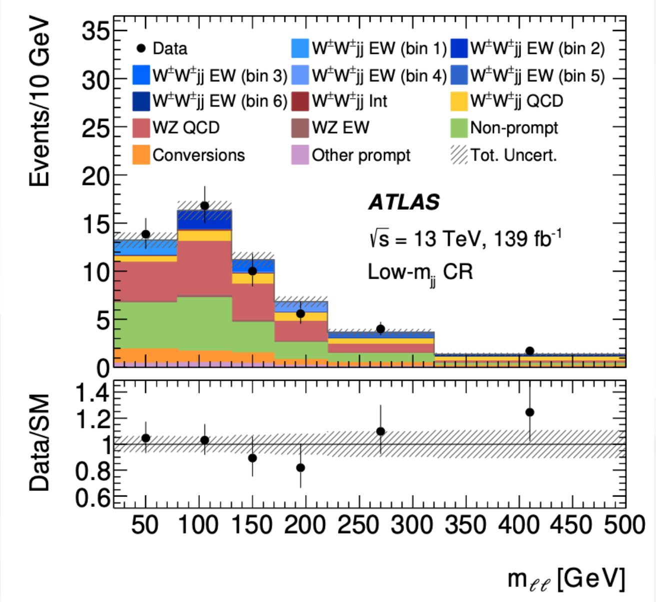

EW(inclusive) $W^{\pm}W^{\pm}jj$ signal strength are extracted in the fiducial region

Description	$\sigma_{\rm fid}^{\rm EW}$ [fb]	$\sigma_{\rm fid}^{\rm EW+Int+QCD}$ [fb]
Measured cross section	2.92 ± 0.22 (stat.) ± 0.19 (syst.)	3.38 ± 0.22 (stat.) ± 0.19 (syst.)
MG5_aMC+Herwig7	2.53 ± 0.04 (PDF) $^{+0.22}_{-0.19}$ (scale)	2.92 ± 0.05 (PDF) $^{+0.34}_{-0.27}$ (scale)
MG5_aMC+Pythia8	2.53 ± 0.04 (PDF) $^{+0.22}_{-0.19}$ (scale)	2.90 ± 0.05 (PDF) $^{+0.33}_{-0.26}$ (scale)
Sherpa	2.48 ± 0.04 (PDF) $^{+0.40}_{-0.27}$ (scale)	2.92 ± 0.03 (PDF) $^{+0.60}_{-0.40}$ (scale)
Sherpa ⊗ NLO EW	2.10 ± 0.03 (PDF) $^{+0.34}_{-0.23}$ (scale)	2.54 ± 0.03 (PDF) $^{+0.50}_{-0.33}$ (scale)
Powheg Box+Pythia	2.64	–

Differential Cross section extraction

$$m_{\rm T} = \sqrt{\left(E_{\rm T}^{\ell\ell} + E_{\rm T}^{\rm miss}\right)^2 - \left|\vec{p}_{\rm T}^{\,\ell\ell} + \vec{E}_{\rm T}^{\rm miss}\right|^2}$$

- m_{ll}, m_{jjj}, m_T, $N_{gapjets}$, ξ_{j_3}(Zeppenfeld)

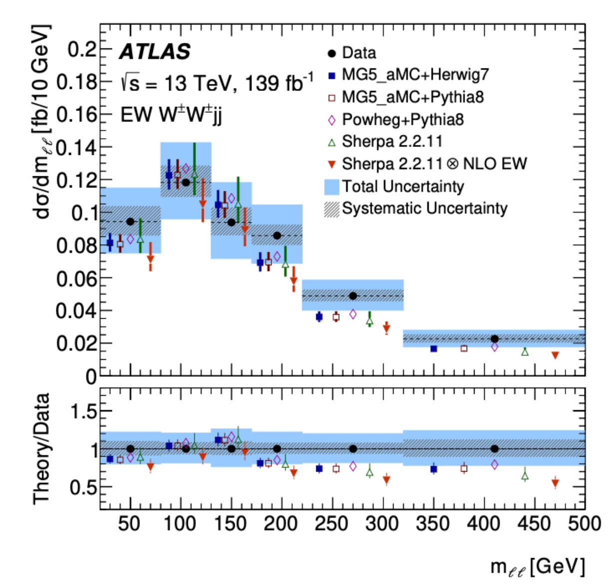

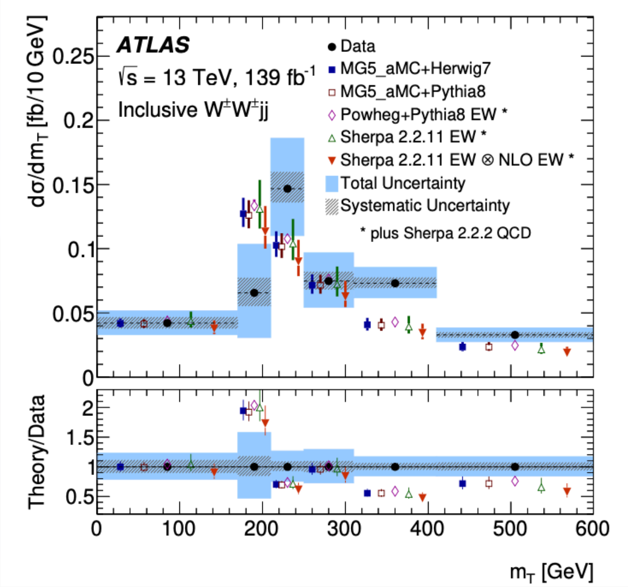

Systematic uncertainties

- non-prompt background estimate(dominant)
- QCD modeling(reweighing m_{jj} to data)

Source	Impact [%]
Experimental	4.6
Electron calibration	0.4
Muon calibration	0.5
Jet energy scale and resolution	1.9
$E_{\rm T}^{\rm miss}$ scale and resolution	0.2
b-tagging inefficiency	0.7
Background, misid. leptons	3.4
Background, charge misrec.	1.0
Pile-up modelling	0.1
Luminosity	1.9
Modelling	4.5
EW $W^{\pm}W^{\pm}jj$, shower, scale, PDF & α_s	0.7
EW $W^{\pm}W^{\pm}jj$, QCD corrections	1.9
EW $W^{\pm}W^{\pm}jj$, EW corrections	0.9
Int $W^{\pm}W^{\pm}jj$, shower, scale, PDF & α_s	0.6
QCD $W^{\pm}W^{\pm}jj$, shower, scale, PDF & α_s	2.6
QCD $W^{\pm}W^{\pm}jj$, QCD corrections	0.8
Background, WZ scale, PDF & α_s	0.3
Background, WZ reweighting	1.5
Background, other	1.3
Model statistical	1.8
Experimental and modelling	6.4
Data statistical	7.4
Total	9.8

$W^\pm W^\pm + jj$: Limits on EFT and H^{++} production

- 3 types of EFT operator related to $W^\pm W^\pm jj$
  - Four Higgs boson covariant derivatives ($O_{S_{0,1,2}}$)
  - Two Higgs boson covariant derivatives and two field-strength tensors ($O_{M_{0,1,7}}$)
  - Four field-strength tensors ($O_{T_{0,1,2}}$)
- Cut-off scale energy scan and 2-D limits
  - Better limits are on O_T

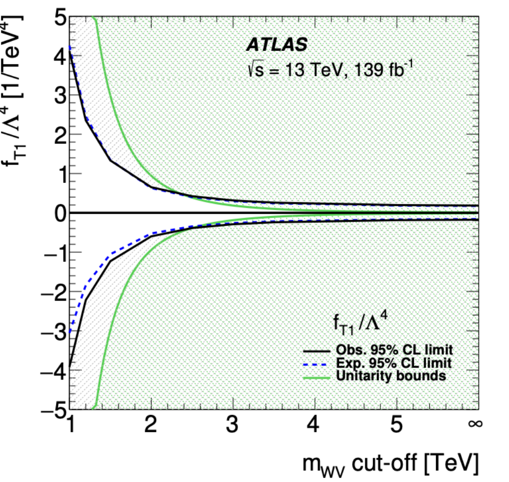

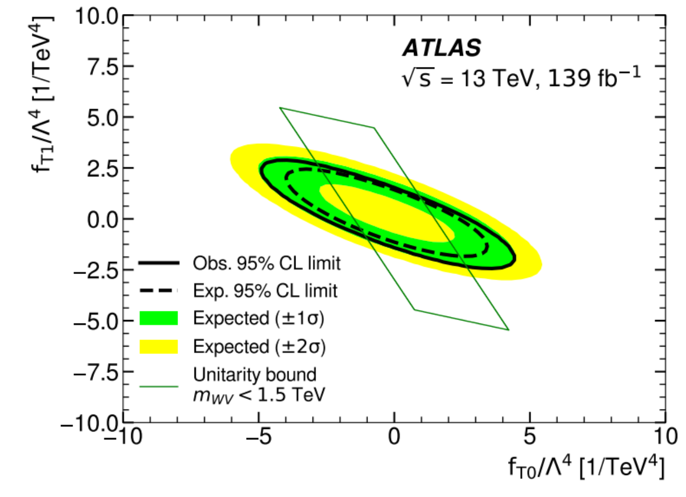

- A quintuplet of fermiophobic Higgs bosons (H±±, H±, and H0) (GM model)
- Excess for the 450GeV mass point (global significance 2.5σ)

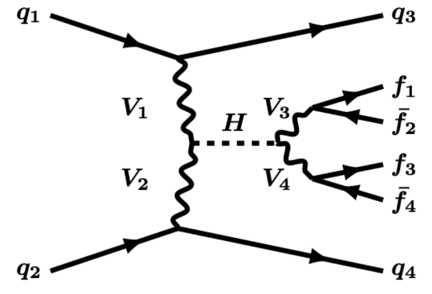

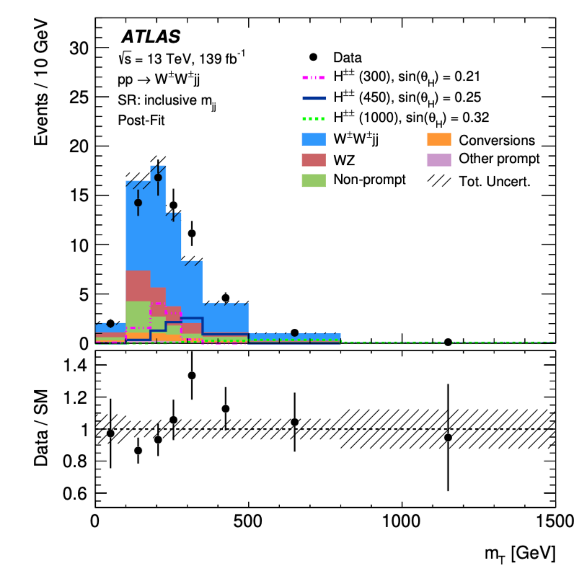

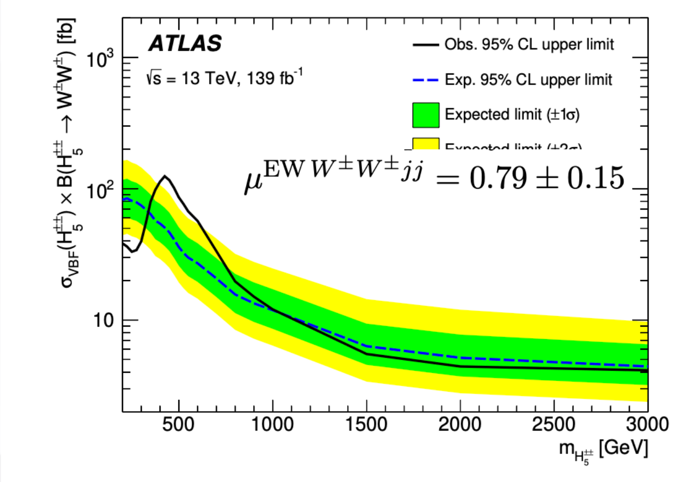

$$\sigma_{\text{VBF}}(\text{H}_5^{\pm\pm}) \times \mathcal{B}(\text{H}_5^{\pm\pm} \to W^\pm W^\pm) = 72 \pm 25 \text{ fb}$$

$$\text{EW } W^\pm W^\pm jj \text{ process } \mu^{\text{EW}\, W^\pm W^\pm jj} = 0.79 \pm 0.15$$

$W^+W^- + jj$: Introduction and selections

arXiv: 2403.04869

- First observation of $EWK\ W^+W^-jj$ (140fb^{-1}) at ATLAS
- **Two neural networks**(final states with 2 jets and 3 jets) are trained to distinguish signal from largest background: top and QCD WW production
- Event selection criteria:

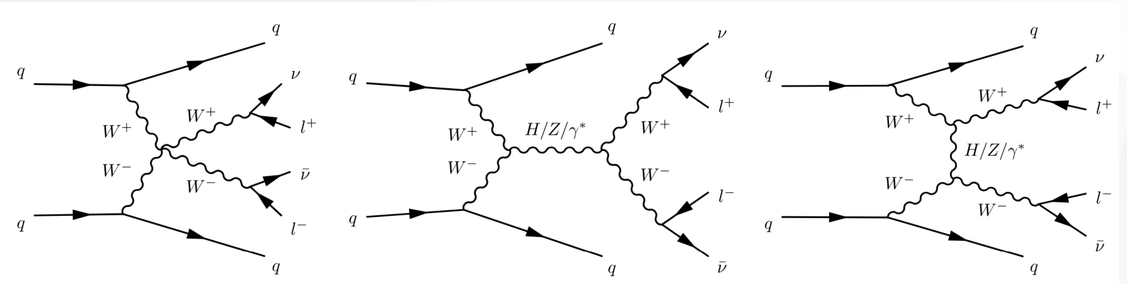

One electron and one muon with opposite electric charges
No additional lepton with $p_T > 10$ GeV, Loose isolation,
Tight/Medium (electrons) and Loose (muons) identification
$m_{e\mu} > 80$ GeV → Suppress Higgs boson mediated W boson pairs via VBF
$E_T^{miss} > 15$ GeV → Reduce Drell-Yan events
No b-jet
Two or three jets
$\zeta > 0.5$

$$\zeta = \text{centrality} = \min\left\{\left[\min(\eta_{\ell_1},\eta_{\ell_2}) - \min(\eta_{j_1},\eta_{j_2})\right], \left[\max(\eta_{j_1},\eta_{j_2}) - \max(\eta_{\ell_1},\eta_{\ell_2})\right]\right\}$$

- Two signal regions: 2 jets and 3 jets (differ by the radiation of an additional gluon)
- Top CR: same cuts as the SR except for requiring one of the two leading jets to be a b-jet.

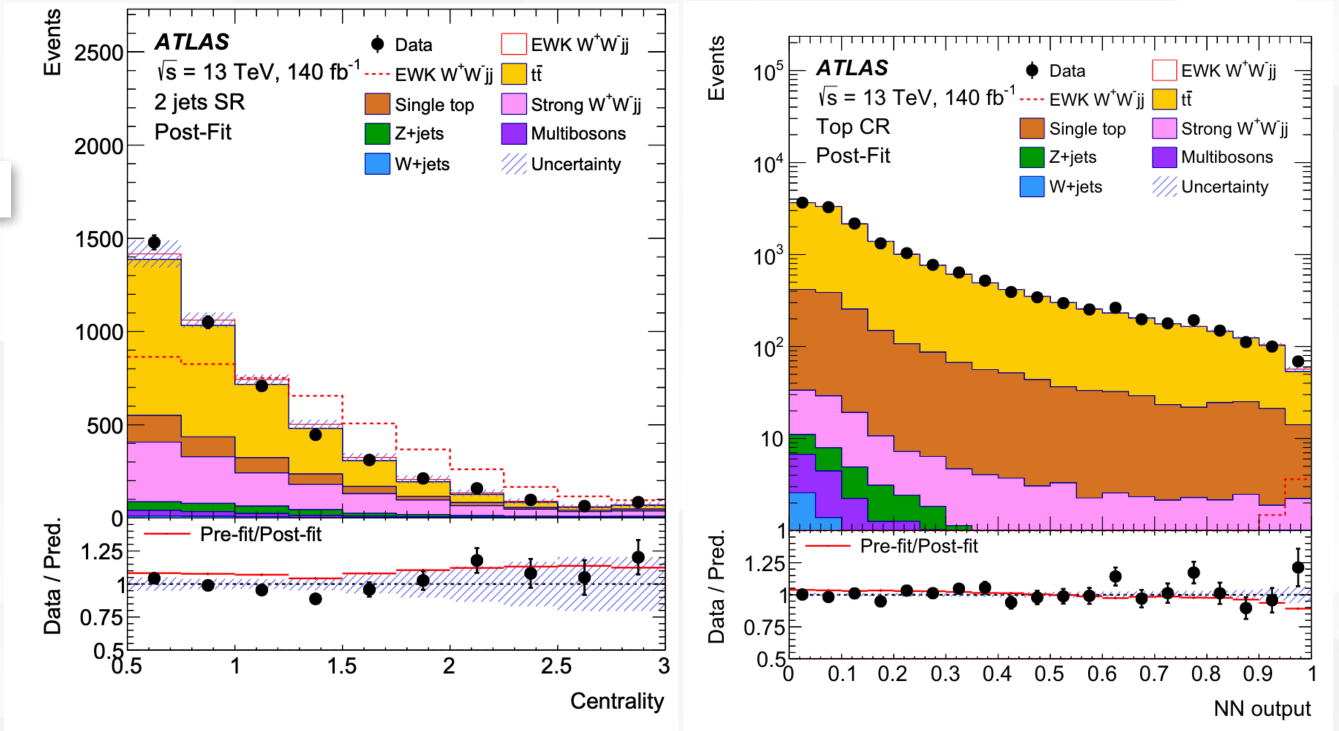

$W^+W^- + jj$: Uncertainties and observed results

arXiv: 2403.04869

- A profile likelihood fit is performed on the NN output observable, simultaneously in SR and CR
- Main uncertainties impact
  - Theoretical: Top quark, EWK, MC stats
  - Experimental: The calibration of jets
- The observed and expected signal significance are **7.1σ and 6.2σ**

Sources	$\frac{\sqrt{(\Delta\mu)^2-(\Delta\mu')^2}}{\mu}$ [%]
MC statistical uncertainty	7.7
Top quark theoretical uncertainties	6.3
Signal theoretical uncertainties	5.8
Jet experimental uncertainties	4.9
Strong W^+W^-jj theoretical uncertainties	1.3
Luminosity	0.8
Misidentified lepton uncertainty	0.5
b-tagging	0.4
Lepton experimental uncertainties	0.1
Others	0.3
Data statistical uncertainty	12.3
Top quark normalisation uncertainty	4.9
Strong W^+W^-jj normalisation uncertainty	2.2
Total uncertainty	18.5

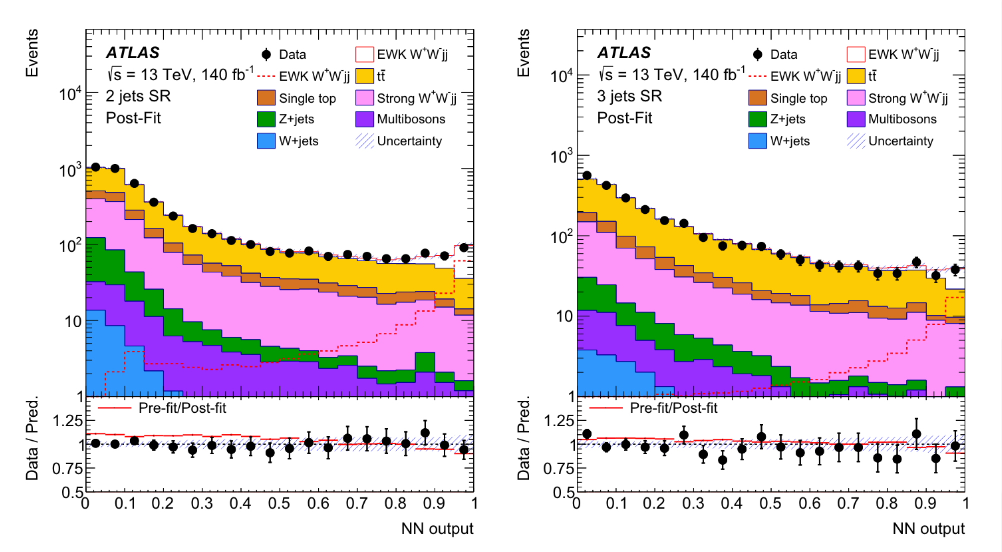

- The signal strength obtained from the fit is: $\mu = 1.21^{+0.23}_{-0.21}$
- The observed(expected) fiducial cross-section is $2.7 \pm 0.5\text{fb}$ $(2.20^{+0.14}_{-0.13}\text{fb})$

Category	Requirements
Leptons	$p_T > 27$ GeV and $\|\eta\| < 2.5$
b-jets	$p_T > 20$ GeV and $\|\eta\| < 2.5$
Jets	$p_T > 25$ GeV and $\|\eta\| < 4.5$
Events	One electron and one muon with opposite electric charges No additional lepton $m_{e\mu} > 80$ GeV $E_T^{miss} > 15$ GeV No b-jet Two or three jets $\zeta > 0.5$ $m_{jj} > 500$ GeV

Fiducial region

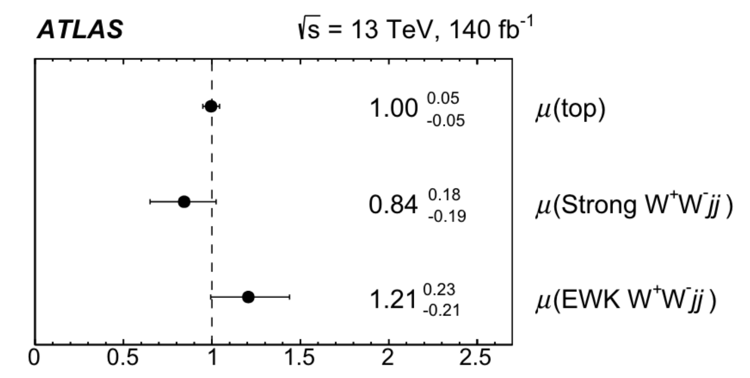

- Integrated and differential cross sections for electroweak and inclusive $W^{\pm}Zjj$ are measured.

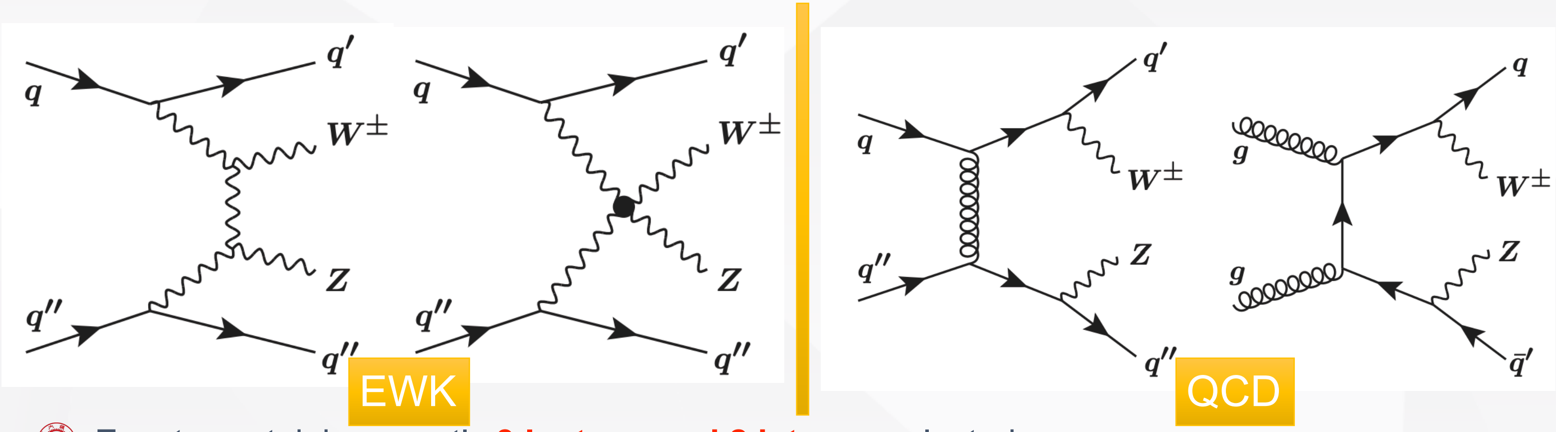

- Events containing exactly **3 leptons and 2 jets** are selected.
- Backgrounds:
  - Dominant irreducible backgrounds are **ZZ** and $\mathbf{t\bar{t} + V}$
  - Reducible backgrounds with non-prompt or fake leptons:

    $Z + jets$, $Z\gamma$, $t\bar{t}$, Wt and WW (**Matrix method**)
- SR($N_{jets} = 2$), SR($N_{jets} >= 3$), b-CR, ZZ-CR
- **BDT**: as final discriminant to separate electroweak and strong $W^{\pm}Zjj$ production modes,

  Adversarial-NN: trained to regress the classification output to reconstruct m_{jj} in order to reduce the modelling uncertainties from m_{jj}.

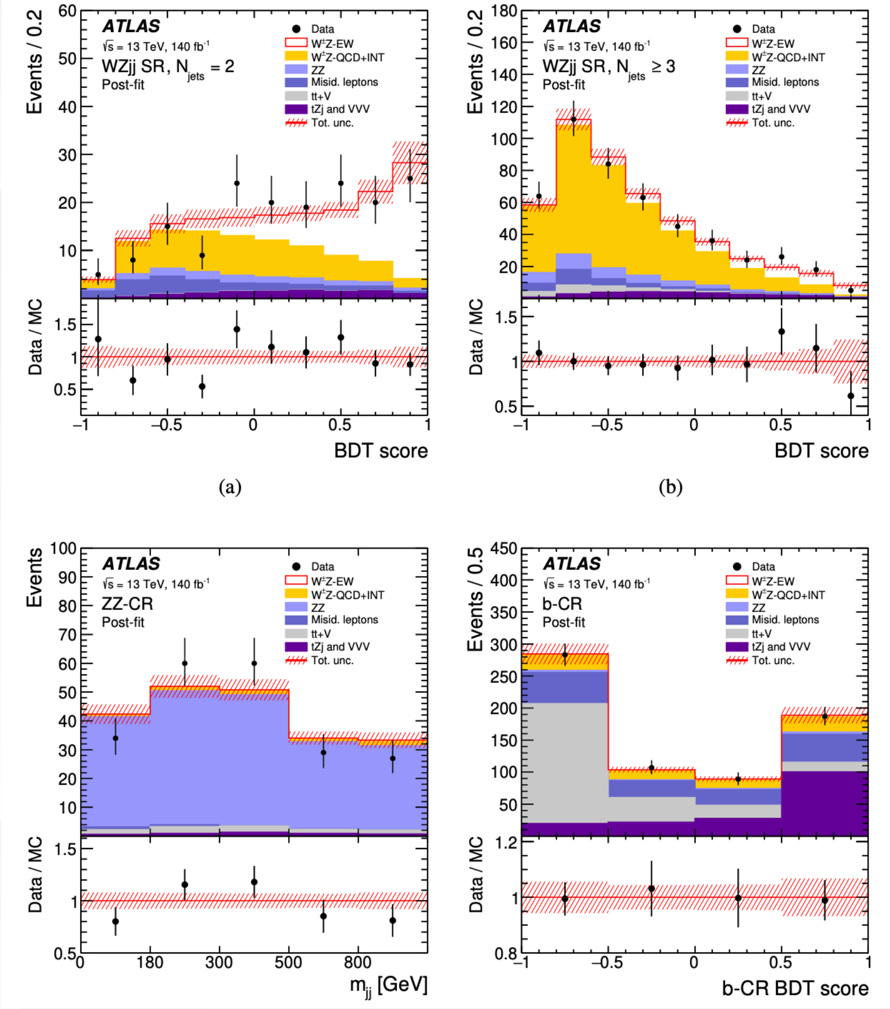

The post-fit distributions in SR and CRs

WZ + jj: Integrated and differential measurements

arXiv: 2403.15296

- $WZjj - EW$ and $WZjj - Strong$ integrated measurements
  - $WZjj - EW$: **A good agreement** of the MC predictions with the measured
  - $WZjj - QCD$: The integrated cross-section is measured to be lower than the prediction from both MC event generators by **a factor of 0.7**

$$
\begin{aligned}
\sigma_{WZjj-\mathrm{EW}} &= 0.368 \pm 0.037\,(\mathrm{stat.}) \pm 0.059\,(\mathrm{syst.}) \pm 0.003\,(\mathrm{lumi.})\ \mathrm{fb} \\
&= 0.37 \pm 0.07\ \mathrm{fb}, \\
\sigma_{WZjj-\mathrm{strong}} &= 1.093 \pm 0.066\,(\mathrm{stat.}) \pm 0.131\,(\mathrm{syst.}) \pm 0.009\,(\mathrm{lumi.})\ \mathrm{fb} \\
&= 1.09 \pm 0.14\ \mathrm{fb},
\end{aligned}
$$

- $WZjj$ differential cross-section measurements
  - sensitive to **aQGC**: Σp_T^l, $\Delta\phi(W,Z)$, m_T^{WZ}
  - the kinematics of **jets**: $N_{jets}^{p_T>40GeV}$, Δy_{jj}, m_{jj}, $\Delta\phi_{jj}$
  - the jet activity in the **gap**: N_{jets}^{gap}, z_{j_3}
  - **BDT score**

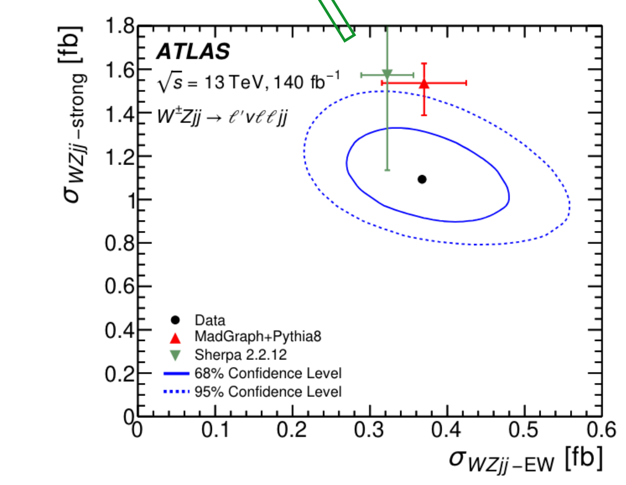

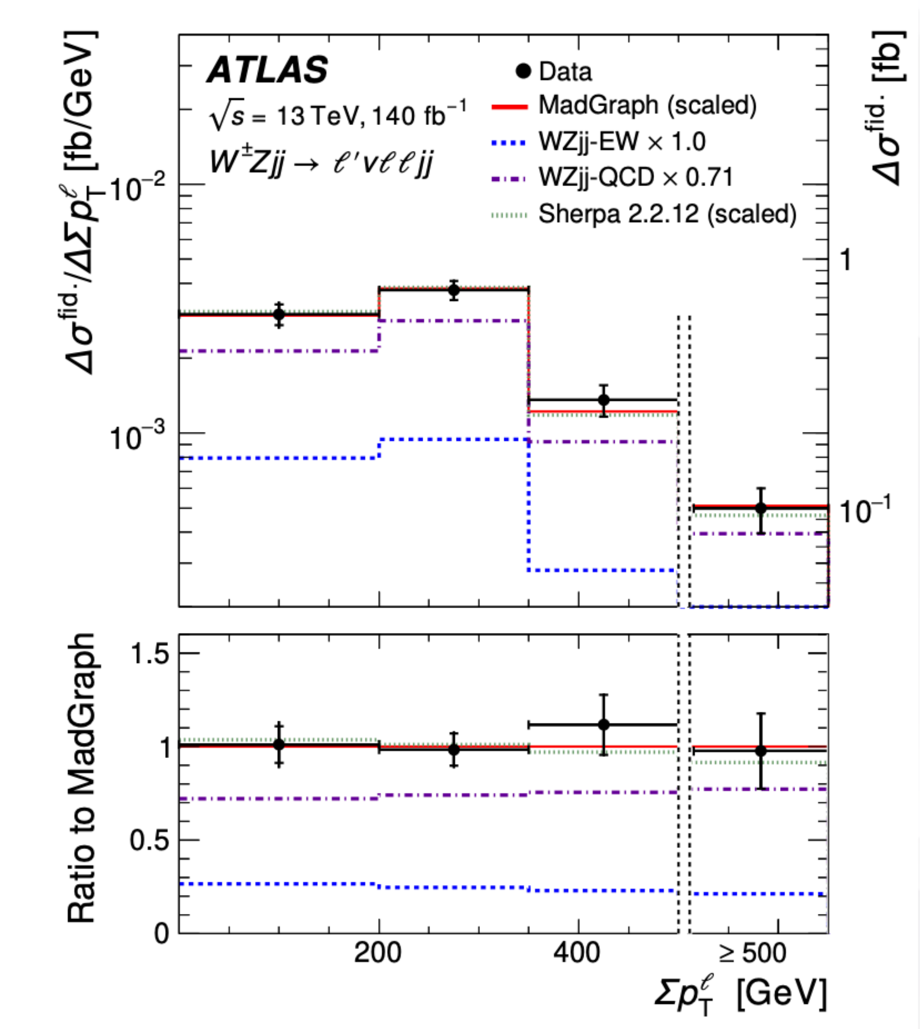

WZ + jj: Dim-8 EFT limits

arXiv: 2403.15296

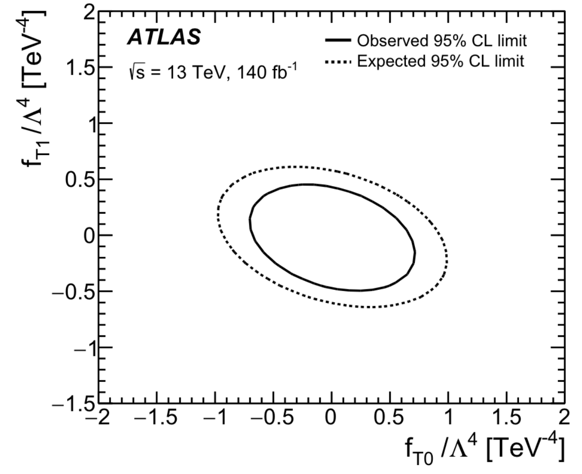

- A two-dimensional combination of the BDT score, separating $WZjj - EW$ from $WZjj - QCD$ events, and m_T^{WZ} observable is used to look for dimension-8 EFT contributions.
- **No deviation with respect to the SM predictions** is observed and the expected and observed 95% confidence level (CL) lower and upper limits on the given Wilson coefficients
- Coefficients associated to the O_{T_0} **and** O_{T_1} operators are the most tight constraint.
- The unitarity bounds from Ref. are used with only one non-zero Wilson coefficient in the m_{WZ} cut-off energy figure.

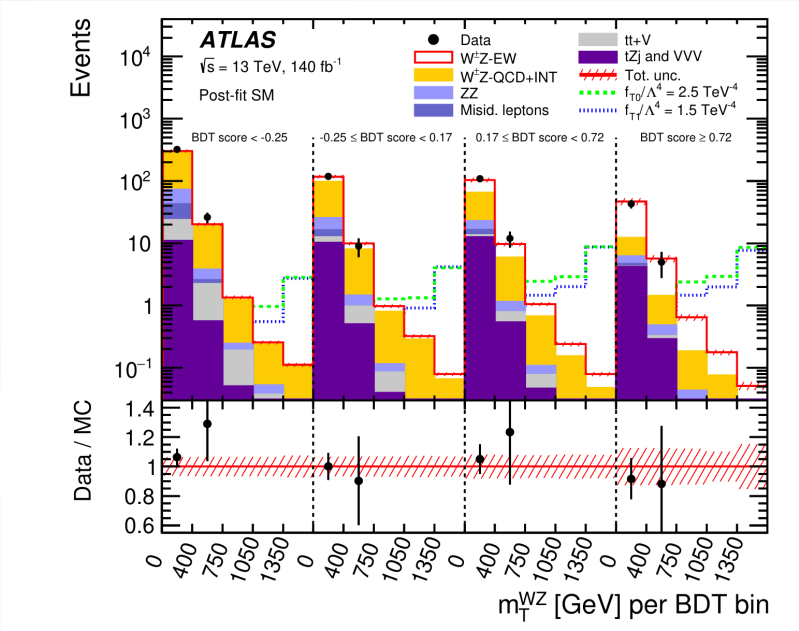

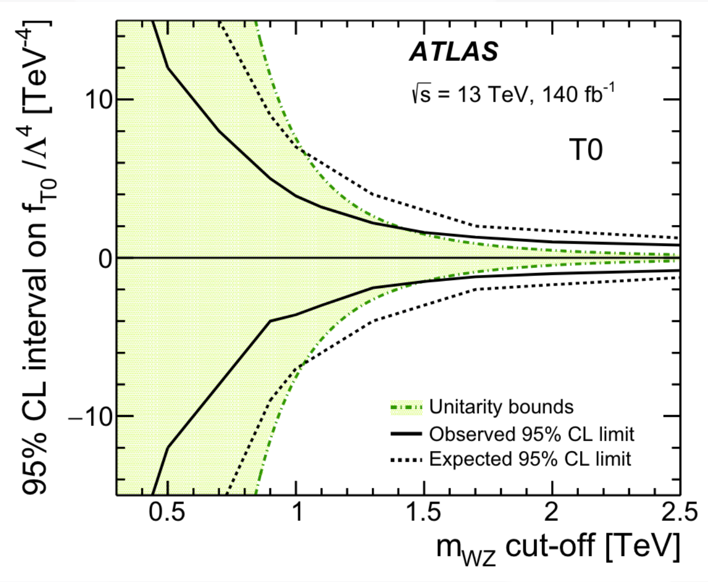

	Expected [TeV $^{-4}$]	Observed [TeV $^{-4}$]
f_{T0}/Λ^4	[-7.0, 7.0]	[-1.5, 1.6]
f_{T1}/Λ^4	[-1.1, 1.0]	[-0.7, 0.6]
f_{T2}/Λ^4	[-12, 6]	[-2.4, 1.8]
f_{M0}/Λ^4	[-60, 60]	[-12, 12]
f_{M1}/Λ^4	[-32, 32]	[-15, 15]
f_{M7}/Λ^4	[-30, 30]	[-15, 15]
f_{S02}/Λ^4	[-41, 41]	[-18, 18]
f_{S1}/Λ^4	—	—

$W\gamma + jj$: Introduction and selections

arXiv: 2403.02809

- Full run2 data at $\sqrt{s} = 13\text{TeV}$ is used
  - To observe $EW\ W\gamma jj$ production
  - To measure a fiducial and differential cross section
- Background estimation
  - Dominated by $QCD\ W\gamma jj$
  - Data-driven methods: $j \to e/\mu, j \to \gamma, e \to \gamma$, pileup
- Neural Network is used to classify signal and background processes.
- SR, CRa, CRb, CRc regions with $m_{jj} > 1000\ \text{GeV}$ are defined for signal extraction.

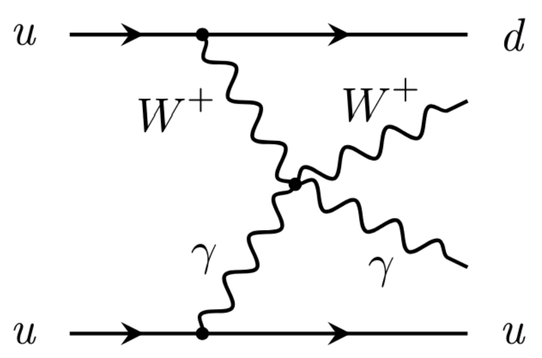

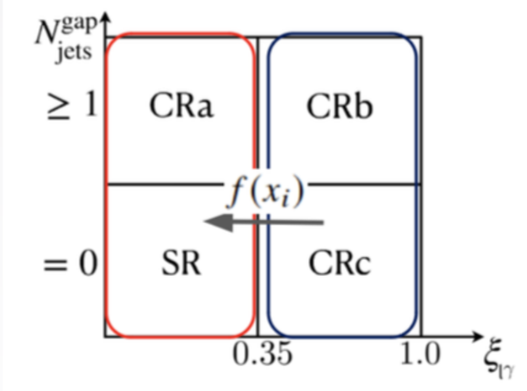

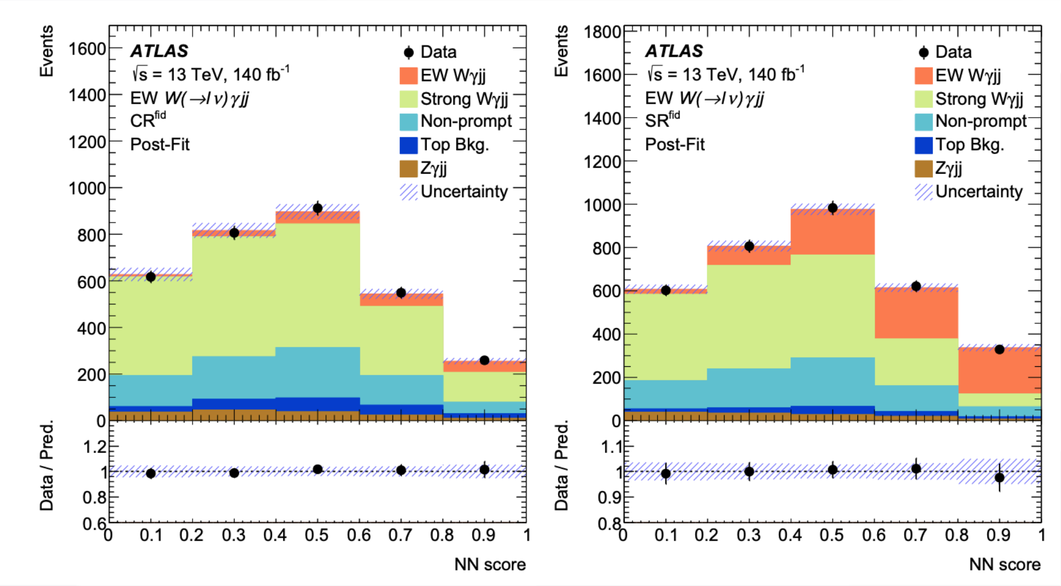

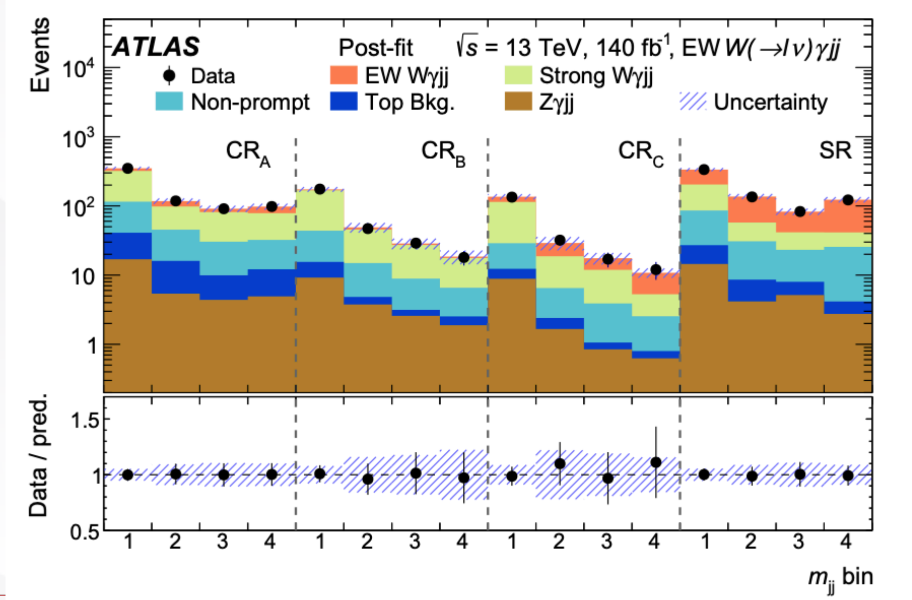

- Signal extraction
  - Observed(expected) significance well **above six standard deviations** (6.3σ)
  - Measured signal strength $\mu_{EW} = 1.5 \pm 0.5$ (using Sherpa)
  - Measured fiducial cross section $\sigma_{EW} = 13.2 \pm 2.5\text{fb}$
- Differential cross section measurements
  - Unfolded using an iterative Bayesian method
  - Measured in M_{jj}, p_{jj}^T, $\Delta\Phi_{jj}$, $M_{l\gamma}$, p_l^T, $\Delta\Phi_{l\gamma}$

Uncertainty Source	Fractional Uncertainty [%]
MC Statistics	11
Jets	8
Lepton, photon, pile-up	8
EW $W\gamma jj$ modelling	7
Data Statistics	6
Strong $W\gamma jj$ modelling	6
Non-prompt background	2
Luminosity	2
Other Background modelling	2
E_T^{miss}	1

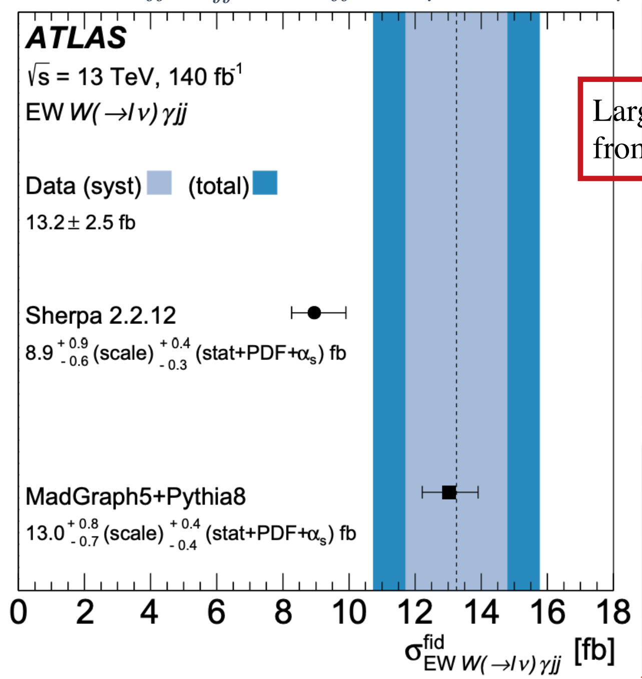

Large signal modeling uncertainty from the choice of event generator

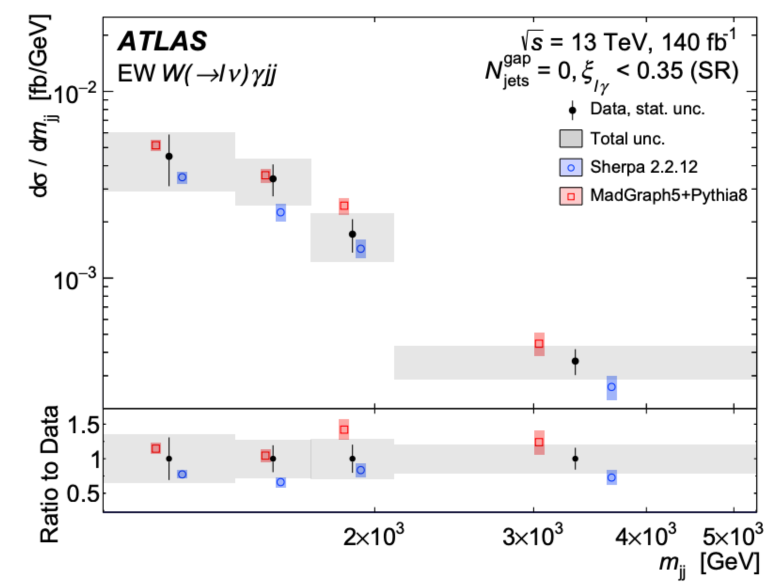

$W\gamma + jj$: EFT interpretation

arXiv: 2403.02809

- The most stringent expected limit on each coefficient is obtained from either the p_{jj}^{T} or p_{l}^{T} distribution.
- The D-8 and interference terms are generated at LO using MadGraph5+Pythia8, with the same PDF and parameter tunes for modeling as the SM terms.
- Clipping technique is used for the limits on the Dim-8 Wilson coefficients.
- The constraints on the f_{T_3} and f_{T_4} operators represent the first such limits at the LHC.

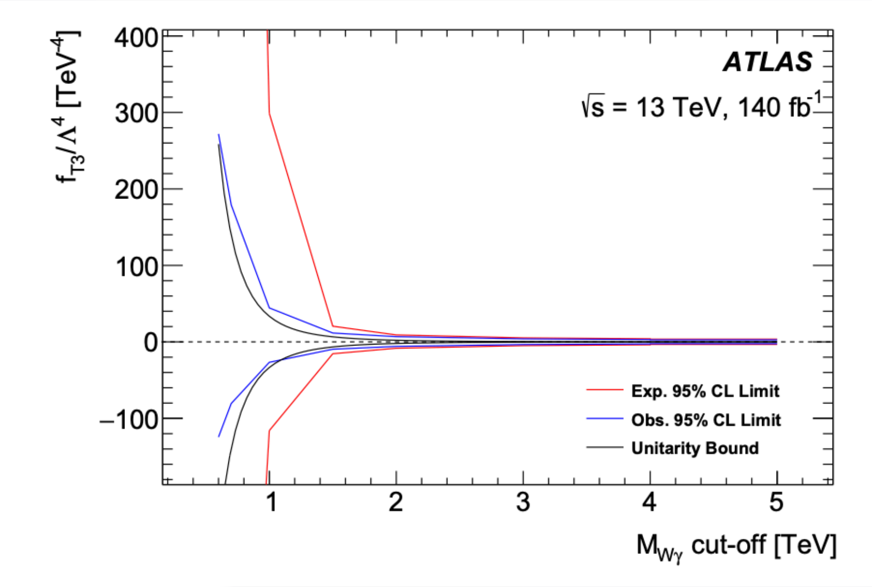

Expected and observed 95% CL limits of the tensor-type operator coupling f_{T_3}

Coefficients [TeV^{-4}]	Observable	$M_{W\gamma}$ cut-off [TeV]	Expected [TeV^{-4}]	Observed [TeV^{-4}]
f_{T0}/Λ^4	p_T^{jj}	-	[-2.4,2.4]	[-1.7,1.8]
f_{T1}/Λ^4	p_T^{jj}	-	[-1.5,1.6]	[-1.1,1.2]
f_{T2}/Λ^4	p_T^{jj}	-	[-4.4,4.7]	[-3.1,3.5]
f_{T3}/Λ^4	p_T^{jj}	-	[-3.3,3.5]	[-2.4,2.6]
f_{T4}/Λ^4	p_T^{jj}	-	[-3.0,3.0]	[-2.2,2.2]
f_{T5}/Λ^4	p_T^{jj}	1.1	[-9.9,9.9]	[-7.5,7.5]
f_{T6}/Λ^4	p_T^{jj}	1.3	[-7.4,7.6]	[-5.2,5.4]
f_{T7}/Λ^4	p_T^{jj}	-	[-3.8,3.9]	[-2.7,2.8]
f_{M0}/Λ^4	p_T^{l}	-	[-38,37]	[-38,37]
f_{M1}/Λ^4	p_T^{l}	-	[-57,58]	[-41,42]
f_{M2}/Λ^4	p_T^{l}	0.8	[-110,110]	[-88,82]
f_{M3}/Λ^4	p_T^{l}	1.1	[-100,110]	[-73,77]
f_{M4}/Λ^4	p_T^{l}	1.0	[-118,111]	[-89,83]
f_{M5}/Λ^4	p_T^{l}	1.3	[-57,80]	[-32,77]
f_{M7}/Λ^4	p_T^{l}	-	[-96,95]	[-69,68]

Expected and observed 95% CL limits for specified $M_{W\gamma}$ cut-off values

Summary

- ATLAS collaboration has made significant advancements in vector boson scattering physics. VBS has proven to be an essential tool for testing the Standard Model and exploring new physics.
- New observation and differential cross section measurements are presented. Limits are set on the corresponding EFT dim-8 operators.
- New analyses underway, stay tuned for Run 3 upcoming results!
  - More data with $\sqrt{s} = 13.6\text{TeV}$
  - Precise theory predictions for signal and background
  - constraints on EFT operators
  - Finding new physical characters via VBS processes

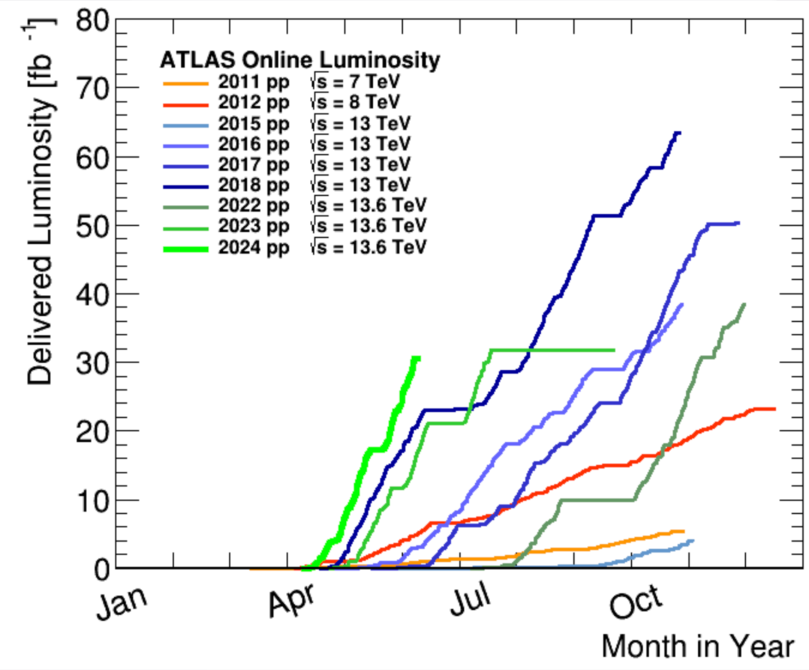

Thanks for your attention

Vector boson scattering in LHC

- Vector-boson reconstruction
  - fully leptonic channels:
    - not large branch ratio for W(20%) and Z(6.7%) , τ leptons not considered due to the secondary decays.
    - cleanest final states and satisfactorily cover the phase spaces of all VBS processes
    - $\mathbf{same-sign\ W^{\pm}W^{\pm}jj}$: golden channel in the study of VBS
  - Semi-leptonic channels:
    - Even larger cross sections but overwhelmingly dominated by single-boson processes ->negligible sensitivity compare to fully leptonic channels
    - Boosted vector bosons $p_T(q\bar{q}) \gtrsim 220\mathrm{GeV}$
    - most stringent limits on the Wilson coefficients of EFT operators
  - Fully hadronic channels:
    - Dominant multi-jet background
    - Two boosted gauge bosons
    - Even better sensitivities than semi-leptonic channels on EFT operators, there are no public LHC analyses

Systematic uncertainties

Source	Uncertainty (%)	
	VBS-enhanced region	VBS-suppressed region
Luminosity	0.8–2.1	0.8–2.0
Leptons	0.8–1.6	1.0–1.5
Jets	2.7–18	3.4–13
Pile-up	0.0–2.5	0.0–0.7
Backgrounds	0.9–9.0	1.2–7.0
Theory modelling	0.6–7.5	1.2–8.8
Unfolding method	0.9–12	1.2–12
Total systematic	6–22	5–17

Differential cross-section measurements

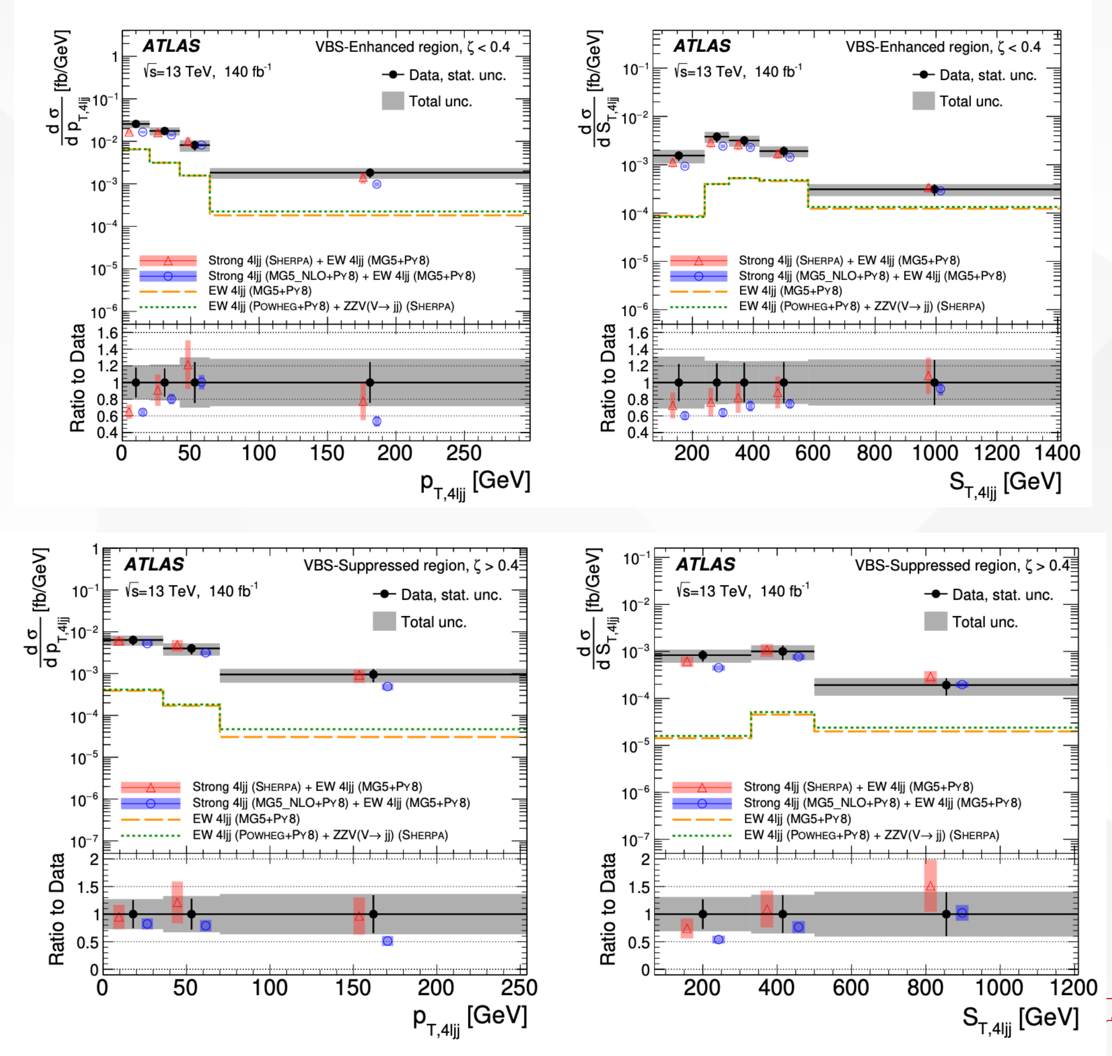

ZZ + jj: Selections

- the centrality of the four-lepton system

$$\zeta = \left| \frac{[y_{4\ell} - 0.5(y_{j_1} + y_{j_2})]}{\Delta y_{jj}} \right|$$

- Selection table

Event Selection	Cut	Requirement
Event Preselection	Trigger	Fire at least one lepton trigger
	Vertex	At least one vertex with 2 or more tracks
Quadruplet Selection	Lepton Kinematics	p_T > 20 GeV for two leading leptons
	Lepton Separation	$\Delta R_{ij} > 0.05$ between leptons in quadruplet
	Pair Requirement	Two SFOS lepton pairs
		$m_{\ell\ell} > 5$ GeV
	Minimal Δm_Z	Select quadruplet with smallest $\lvert m_{12} - m_Z\rvert + \lvert m_{34} - m_Z\rvert$
		Leading Pair: pair with highest $\lvert y_{ij}\rvert$
	ZZ Mass	$m_{4\ell} > 130$ GeV
Quadruplet Categorisation	Signal Quadruplet	All leptons in quadruplet are **signal leptons**
	Not-Signal Quadruplet	At least one lepton in quadruplet are **baseline-not-signal lepton**
Dijet Selection	Different Detector Sides	$\eta_{j1} \times \eta_{j2} < 0$
	Rapidity Separation	$\Delta Y_{jj} > 2$
	Leading Jet p_T	$p_{T,j1} > 40$ GeV
	Dijet Mass	$m_{jj} > 300$ GeV
	Signal Region Dijet	Both jets required to pass either JVT or FJVT
Event Categorisation	VBS Enhanced Region	signal quadruplet, signal dijet & centrality (ζ) < 0.4
	VBS Suppressed Region	signal quadruplet, signal dijet & centrality (ζ) > 0.4

$W^{\pm}W^{\pm}$ + jj: Limits on EFT

JHEP04(2024)026

Expected and observed limits on the Wilson coefficients

Coefficient	Type	No unitarisation cut-off [TeV^{-4}]	Lower, upper limit at the respective unitarity bound [TeV^{-4}]
f_{M0}/Λ^4	Exp.	[-3.9, 3.8]	-64 at 0.9 TeV, 40 at 1.0 TeV
	Obs.	[-4.1, 4.1]	-140 at 0.7 TeV, 117 at 0.8 TeV
f_{M1}/Λ^4	Exp.	[-6.3, 6.6]	-25.5 at 1.6 TeV, 31 at 1.5 TeV
	Obs.	[-6.8, 7.0]	-45 at 1.4 TeV, 54 at 1.3 TeV
f_{M7}/Λ^4	Exp.	[-9.3, 8.8]	-33 at 1.8 TeV, 29.1 at 1.8 TeV
	Obs.	[-9.8, 9.5]	-39 at 1.7 TeV, 42 at 1.7 TeV
f_{S02}/Λ^4	Exp.	[-5.5, 5.7]	-94 at 0.8 TeV, 122 at 0.7 TeV
	Obs.	[-5.9, 5.9]	–
f_{S1}/Λ^4	Exp.	[-22.0, 22.5]	–
	Obs.	[-23.5, 23.6]	–
f_{T0}/Λ^4	Exp.	[-0.34, 0.34]	-3.2 at 1.2 TeV, 4.9 at 1.1 TeV
	Obs.	[-0.36, 0.36]	-7.4 at 1.0 TeV, 12.4 at 0.9 TeV
f_{T1}/Λ^4	Exp.	[-0.158, 0.174]	-0.32 at 2.6 TeV, 0.44 at 2.4 TeV
	Obs.	[-0.174, 0.186]	-0.38 at 2.5 TeV, 0.49 at 2.4 TeV
f_{T2}/Λ^4	Exp.	[-0.56, 0.70]	-2.60 at 1.7 TeV, 10.3 at 1.2 TeV
	Obs.	[-0.63, 0.74]	–

Table 8. Expected and observed limits on the Wilson coefficients for various operators without any unitarisation procedure and with a unitarisation cut-off at the unitarity bound. The last column represents lower and upper limits at the respective cut-off value, where the unitarity bound and experimental bound cross. Cases where no crossing with the unitarity bound was found in the scanned region above 600 GeV are labelled by "–". The notation S02 is used to indicate that the coefficients corresponding to the operators O_{S0} and O_{S2} are assigned the same value. The limits on M7 are obtained without taking into account the SM-EFT interference for the EW $W^{\pm}Zjj$ final state.

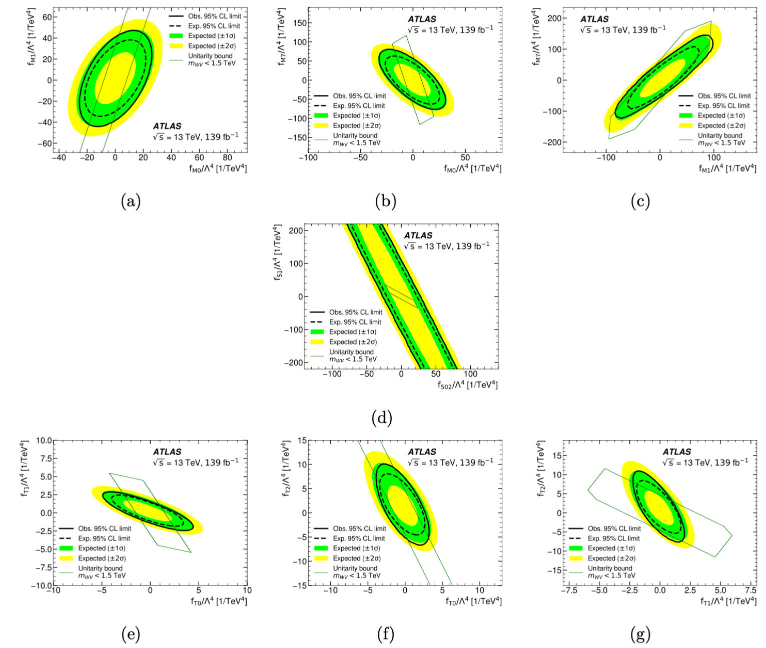

Figure 10. Two-dimensional median expected (dashed line) and observed (solid line) 95% CL intervals on parameters corresponding to the quartic operator combinations (a) M0-M1, (b) M0-M7, (c) M1-M7, (d) S1-S02, (e) T0-T1, (f) T0-T2 and (g) T1-T2 EFT parameters with a unitarisation cut-off scale of 1.5 TeV and unitarity bounds (green line). The two-dimensional unitarity bounds for pairs of operators are obtained for the two non-zero Wilson coefficients from the eigenvalues from ref. [99]. The 1 (green) and 2 (yellow) sigma bands show the 68.3% and 95.4% CL regions for the expected limit curves, respectively. The limits on M7 are obtained without taking into account the SM-EFT interference term and EFT cross-term for the EW $W^{\pm}Zjj$ final state.

$W^{\pm}W^{\pm} + jj$: Differential measurements and uncertainties

- The agreement is worse for mT where an overprediction of the data in the region 170 < mT < 210 GeV and underprediction in the region 310 < mT < 410 GeV are observed, which follow the behaviour at the reconstructed level.

Variable	EW $W^{\pm}W^{\pm}jj$		Inclusive $W^{\pm}W^{\pm}jj$		Max. value in data
	χ^2/N_{dof}	p-value	χ^2/N_{dof}	p-value	
$m_{\ell\ell}$	4.5/6	0.605	7.34/6	0.291	1081 GeV
m_{T}	13.0/6	0.043	16.33/6	0.012	1270 GeV
m_{jj}	7.6/6	0.266	8.67/6	0.193	6328 GeV
$N_{\text{gap jets}}$	2.5/2	0.282	2.53/2	0.282	5
ξ_{j3}	4.2/5	0.517	4.93/5	0.424	1.74

Table 7. χ^2 and p-values obtained from the measured differential cross sections and the nominal MG5_aMC+Herwig7 prediction, computed using the covariance matrix of the measured differential cross section and the difference between data and model. The number of degrees of freedom N_{dof} is equal to the number of the cross section bins. The uncertainties in the MC prediction are ignored when computing χ^2 and p-values. The values are provided for both EW and inclusive differential $W^{\pm}W^{\pm}jj$ cross sections. The last column shows the maximum value of the respective variable observed in data.

WZ + jj: Additional differential cross section results

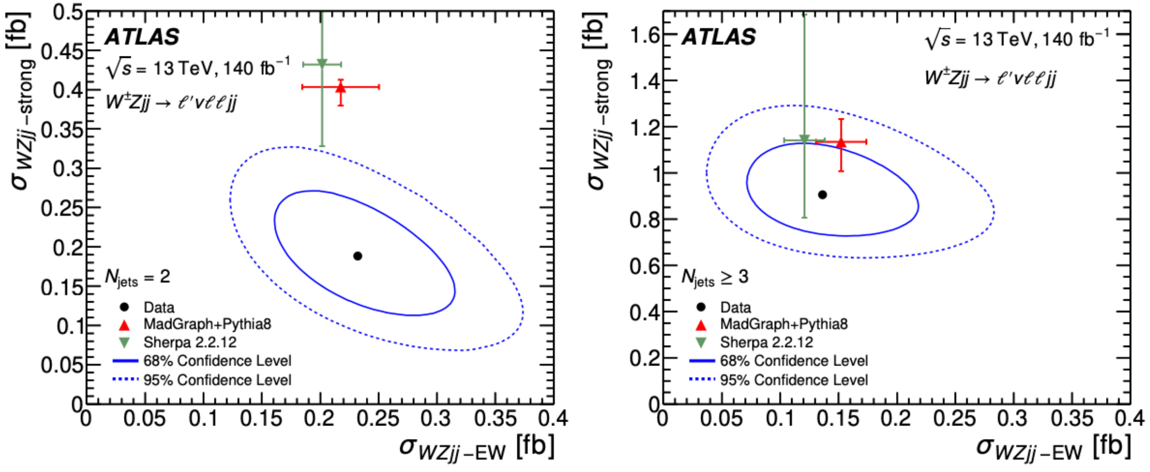

(a) (b)

Figure 5: The measured $\sigma_{WZjj-\mathrm{EW}}$ and $\sigma_{WZjj-\mathrm{strong}}$ cross-sections (a) for $N_{\mathrm{jets}} = 2$ and (b) $N_{\mathrm{jets}} \geq 3$ compared with predictions from MadGraph+Pythia8 (upward pointing triangle) and Sherpa 2.2.12 (downward pointing triangle). The full and dashed contours around the data points correspond to 68% and 95% CL, respectively.

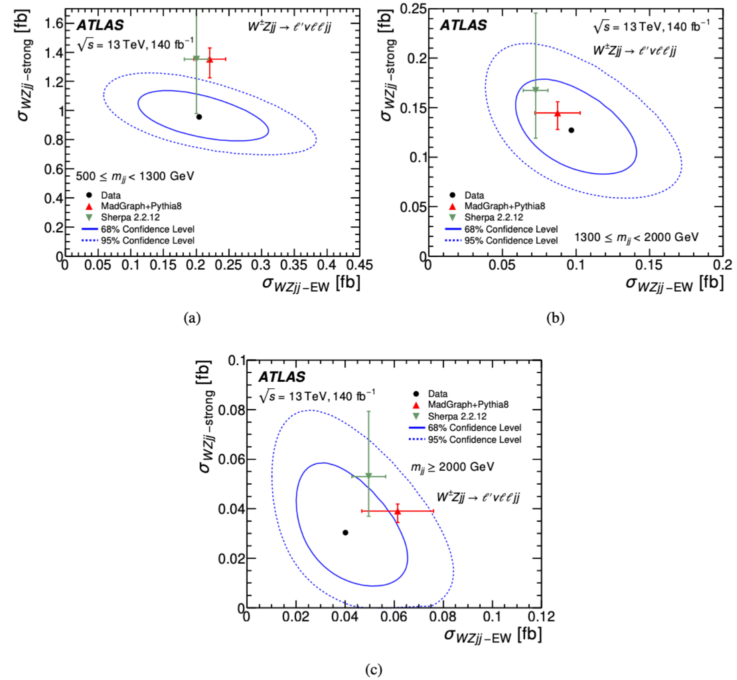

Figure 6: The measured $\sigma_{WZjj-\mathrm{EW}}$ and $\sigma_{WZjj-\mathrm{strong}}$ cross-sections per m_{jj} bin, (a) $500 \leq m_{jj} < 1300$ GeV, (b) $1300 \leq m_{jj} < 2000$ GeV, (c) $m_{jj} \geq 2000$ GeV, compared with predictions from MadGraph+Pythia8 (upward pointing triangle) and Sherpa 2.2.12 (downward pointing triangle). The full and dashed contours around the data points correspond to 68% and 95% CL, respectively.

Cross sections for different regions

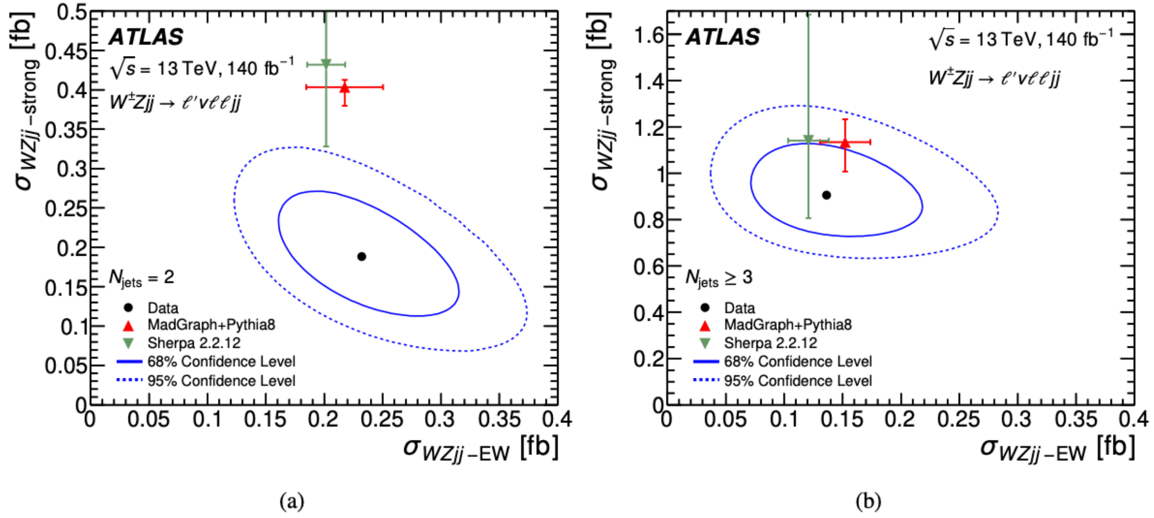

Figure 5: The measured $\sigma_{WZjj-\text{EW}}$ and $\sigma_{WZjj-\text{strong}}$ cross-sections (a) for $N_{\text{jets}} = 2$ and (b) $N_{\text{jets}} \geq 3$ compared with predictions from MadGraph+Pythia8 (upward pointing triangle) and Sherpa 2.2.12 (downward pointing triangle). The full and dashed contours around the data points correspond to 68% and 95% CL, respectively.

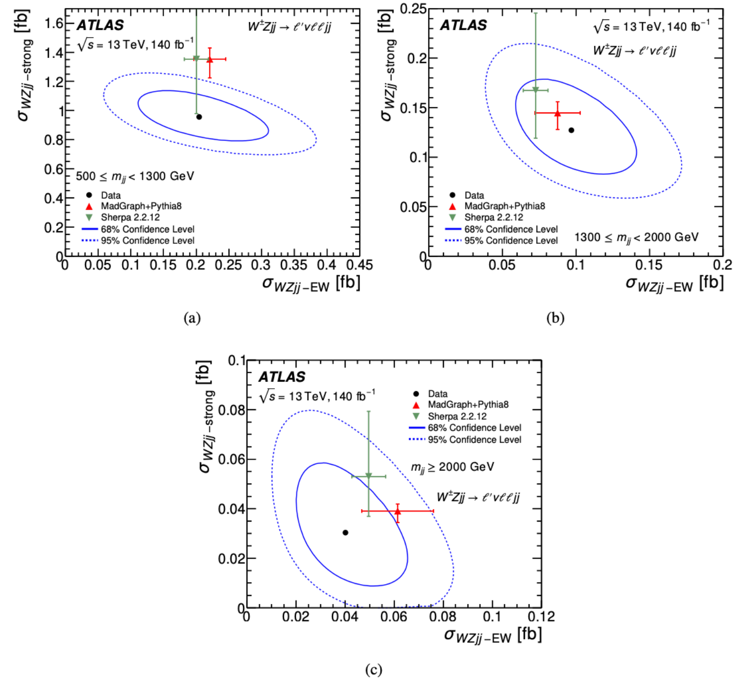

Figure 6: The measured $\sigma_{WZjj-\text{EW}}$ and $\sigma_{WZjj-\text{strong}}$ cross-sections per m_{jj} bin, (a) $500 \leq m_{jj} < 1300$ GeV, (b) $1300 \leq m_{jj} < 2000$ GeV, (c) $m_{jj} \geq 2000$ GeV, compared with predictions from MadGraph+Pythia8 (upward pointing triangle) and Sherpa 2.2.12 (downward pointing triangle). The full and dashed contours around the data points correspond to 68% and 95% CL, respectively.

$W\gamma$ + jj: Fiducial regions

Definition of fiducial regions

Table 1: Summary table for signal and control regions for the fiducial and differential cross-section measurements.

Fiducial cross-section	SR^{fid}		CR^{fid}	
	$N_{jets}^{gap} = 0$		$N_{jets}^{gap} > 0$	
Differential cross-section	SR	CR_A	CR_B	CR_C
$m_{jj} > 1$ TeV	$N_{jets}^{gap} = 0$ $\xi_{l\gamma} < 0.35$	$N_{jets}^{gap} > 0$ $\xi_{l\gamma} < 0.35$	$N_{jets}^{gap} > 0$ $0.35 < \xi_{l\gamma} < 1$	$N_{jets}^{gap} = 0$ $0.35 < \xi_{l\gamma} < 1$

	SR^{fid} $\left(N_{jets}^{gap} = 0\right)$	CR^{fid} $\left(N_{jets}^{gap} > 0\right)$
EW $W\gamma jj$	520 ± 141	120 ± 49
Strong $W\gamma jj$	1550 ± 830	1970 ± 950
Non-prompt	692 ± 57	698 ± 58
Top quark processes	109 ± 18	183 ± 37
EW + strong $Z\gamma jj$	128 ± 34	163 ± 77
Total	3000 ± 830	3140 ± 960
Data	3341	3143

Table 3: Particle-level definition for the fiducial and differential EW $W\gamma jj$ measurement.

Object	Selection requirements
Dressed muons	$p_T > 30$ GeV and $\|\eta\| < 2.5$
Dressed electrons	$p_T > 30$ GeV and $\|\eta\| < 2.47$ (excluding $1.37 < \|\eta\| < 1.52$)
Isolated photons	$E_T^{\gamma} > 22$ GeV and $\|\eta\| < 2.37$ (excluding $1.37 < \|\eta\| < 1.52$) and $E_T^{iso} < 0.2E_T^{\gamma}$
Jets	At least two jets with $p_T > 50$ GeV and $\|y\| < 4.4$, b–jet veto
Missing transverse momentum	$E_T^{miss} > 30$ GeV and $m_T^W > 30$ GeV
VBS topology	$N_\ell = 1$, $N_\gamma \geq 1$, $\|m_{\ell\gamma} - m_Z\| > 10$ GeV $\Delta R_{min}(\ell, j) > 0.4$, $\Delta R_{min}(\gamma, j) > 0.4$, $\Delta R_{min}(\ell, \gamma) > 0.4$ $\Delta R_{min}(j_1, j_2) > 0.4$, $\Delta\phi_{min}(E_T^{miss}, j) > 0.4$ $N_{jets} \geq 2$, $p_T^{j1}, p_T^{j2} > 50$ GeV $m_{jj} > 500$ GeV, $\|\Delta y_{jj}\| > 2$
Fiducial measurement	VBS topology
Differential measurement	VBS topology $\oplus$ ($m_{jj} > 1000$ GeV, $N_{jets}^{gap} = 0$, and $\xi_{W\gamma} < 0.35$)